Final Report

Cyanate Ester Composite Resins Derived from Renewable Polyphenol Sources

SERDP Project Number: **WP-1759**

Performing Organization: US Navy, NAVAIR
Naval Air Warfare Center, Weapons Division
Research Division, Chemistry Department
1900 N. Knox Road, Stop 6303
China Lake, CA 93555-6106

Lead Principal Investigator: Dr. Benjamin G. Harvey
760-939-0247 (phone)
760-939-1617 (fax)
e-mail: benjamin.g.harvey@navy.mil

Date: 03/16/2011

REPORT DOCUMENTATION PAGE

Form Approved
OMB No. 0704-0188

1. REPORT DATE *(DD-MM-YYYY)*	2. REPORT TYPE	3. DATES COVERED *(From - To)*
03/16/2011	Final Report	01/2010 to 03/2011

4. TITLE AND SUBTITLE
Cyanate Ester Composite Resins Derived from Renewable Polyphenol Sources

5a. CONTRACT NUMBER

5b. GRANT NUMBER

5c. PROGRAM ELEMENT NUMBER

6. AUTHOR(S)
Benjamin G. Harvey, Michael E. Wright, Andrew G. Guenthner, Scott Compel, Matthew Davis, Kevin Lamison, Lee Cambrea, Heather Meylemans, Sean McCormick, Thomas Groshens, Lawrence Baldwin, Michael Ford, Shannon Haines, and Jessica Cash

5d. PROJECT NUMBER
10 WP03-020 / WP-1759

5e. TASK NUMBER

5f. WORK UNIT NUMBER

7. PERFORMING ORGANIZATION NAME(S) AND ADDRESS(ES)
US Navy, NAVAIR; Naval Air Warfare Center, Weapons Division
Research Division, Chemistry Department
1900 N. Knox Road, Stop 6303
China Lake, CA 93555

8. PERFORMING ORGANIZATION REPORT NUMBER

9. SPONSORING/MONITORING AGENCY NAME(S) AND ADDRESS(ES)
Strategic Environmental Research and Development Program

10. SPONSOR/MONITOR'S ACRONYM(S)
SERDP

11. SPONSOR/MONITOR'S REPORT NUMBER(S)

12. DISTRIBUTION/AVAILABILITY STATEMENT
Distribution Statement A

13. SUPPLEMENTARY NOTES

14. ABSTRACT
Cyanate ester resins were synthesized from a series of renewable phenols including; vanillin, creosol, resorcylic acid, resveratrol, and nordihydroguarietic acid. These phenols can be derived from plant sources and even waste biomass, allowing for high performance resins to be produced in an environmentally responsible manner. The physical properties, cure chemistry, thermal stability and high temperature decomposition mechanisms of the resins were rigorously studied and promising candidates were used in the fabrication of test panels on both glass and carbon fiber supports. The impressive physical characteristics of these sustainable resins suggest that they are good candidates for a variety of DoD applications.

15. SUBJECT TERMS
Renewable Composites, Cyanate Esters, High Performance Polymers, Green Chemistry

16. SECURITY CLASSIFICATION OF:			17. LIMITATION OF ABSTRACT	18. NUMBER OF PAGES	19a. NAME OF RESPONSIBLE PERSON
a. REPORT	b. ABSTRACT	c. THIS PAGE			Benjamin G. Harvey
					19b. TELEPHONE NUMBER *(Include area code)*
UU	UU	UU	SAR	50	760-939-0247

Table of Contents

List of Figures iv

List of Schemes vi

List of Tables vii

List of Symbols, Abbreviations, and Acronyms viii

Acknowledgements ix

1. Abstract 1

2. Objective 2

3. Background 3

4. Materials and Methods 7
   - 4.1 Chemical Synthesis 7
     - 4.1.1 General methods 7
     - 4.1.2 Chloroform extraction of creosote leaves and stems 7
     - 4.1.3 Isolation of NDGA from creosote leaves and stems 7
     - 4.1.4 Preparation of a cyanate ester from NDGA 7
     - 4.1.5 Preparation f 3,3'-dimethoxy-5,5'-dimethyl-[1,1'-biphenyl]-2,2'-diol (1) 8
     - 4.1.6 Preparation of 2,2'-dicyanato-3,3'-dimethoxy-5,5'-dimethyl-1,1'-biphenyl (2) 8
     - 4.1.7 Preparation of 2,2'-bis(cyanato)-1,1'-biphenyl (3) 8
     - 4.1.8 Preparation of 2,2'-bis(cyanato)-1,1'-binaphthyl (4) 8
     - 4.1.9 Preparation of (*E*)-4,4'-(ethane-1,2-diyl)bis(2-methoxyphenol) (5) 8
     - 4.1.10 Preparation of 4,4'-(ethane-1,2-diyl)bis(2-methoxyphenol) (6) 9
     - 4.1.11 Preparation of (*E*)-1,2-bis(4-cyanato-3-methoxyphenyl)ethene (7) 9
     - 4.1.12 Preparation of 1,2-bis(4-cyanato-3-methoxyphenyl)ethane (8) 9
     - 4.1.13 Preparation of 5-(2-ethylhexyloxy)resorcinol (9) 9
     - 4.1.14 Preparation of 5-(2-ethylhexyloxy)-1,3-bis(cyanato)benzene (10) 10
     - 4.1.15 Preparation of methyl 3,5-bis(cyanato)benzoate (11) 10
     - 4.1.16 Preparation of propyl 3, 5-bis(cyanato)benzoate (12) 10
     - 4.1.17 Preparation of trans 3,4'-5-tricyanatostilbene (13) 10
     - 4.1.18 Preparation of diethyl 4-methoxybenzylphophonate (14) 11
     - 4.1.19 Preparation of *trans*-3,4',5-trimethoxystilbene (15) 11
     - 4.1.20 Preparation of 3,4',5-trimethoxydibenzyl (16) 11
     - 4.1.21 Preparation of 3,4',5-trihydroxydibenzyl (17) 12
     - 4.1.22 Preparation of 3,4',5-tricyanatodibenayl (18) 12
     - 4.1.23 Preparation of trans-4,4'-dicyanatostilbene (19) 12
     - 4.1.24 Preparation of 4,4'-dihydroxydibenzyl (20) 12
     - 4.1.25 Preparation of 4,4'-dicyanatodibenzyl (21) 12

4.1.26 Preparation of 4,4'-dihydroxydeoxybenzoin (22)....12
4.1.27 Preparation of 4,4'-dicyantodeoxybenzoin (23)....13
4.1.28 Preparation of 1,3-dicyanato-5-(4-cyanatophenethyl)benzene (24)....13
4.2 Characterization and Analysis....13
4.2.1 Test sample preparations....13
4.2.2 Physical analysis....13
4.2.3 Analysis by TGA/FTIR....14
4.2.4 Differential Scanning Calorimetry (DSC) at AFRL....14
4.2.5 Oscillatory Thermomechanical Analysis (OTMA) at AFRL....14
4.2.6 Density measurements....14
4.2.7 Hot water exposure testing....15
4.3 Composite Fabrication....15
4.3.1 Materials....15
4.3.2 Laminate fabrication....15
5. Results & Discussion....16
5.1 Cyanate Esters from Creosote Bush Extract....16
5.2 Vanillin as a Feedstock for High Performance Cyanate Esters....18
5.3 Synthesis of *bis*-Phenols and Corresponding Cyanate Esters....18
5.4 Solid State Structures of Selected *bis*-Cyanate Esters....19
5.5 *bis*-(Vanillin Cyanate Ester) Curing Chemistry....21
5.6 Summary of Vanillin Work....26
5.7 Single Ring bis-Cyanate Esters from Resorcylic Acid....26
5.7.1 Synthesis of *bis*-cyanate esters....26
5.7.2 Material testing (density, water uptake)....27
5.7.3 Thermal analysis of single-ring cyanate esters....27
5.7.4 Single ring cyanate ester composites....33
5.7.5 Summary of resorcylic acid derived cyanate esters....34
5.8 Renewable tricyanate esters....35
6. Concluding Remarks....38
6.1 Project Summary....38
6.2 Future Directions....39
6.2.1 Vanillin derived resins....39
6.2.2 Resorcylic acid based resins....39
6.2.3 Tricyanate ester resins....39
7. References....40

List of Figures

Figure 1. Typical petroleum-based dicyanate ester monomer. 4

Figure 2. Selected structures of renewable phenolics examined in this work. 4

Figure 3. Graphical depiction of lignin. 6

Figure 4. FTIR of the chloroform extract of creosote leaves and stems (top) and residual oil after treatment with cyanogens bromide and triethylamine (bottom). 16

Figure 5. FTIR spectrum of NDGA (top) and NDGA treated with cyanogen bromide and triethylamine (bottom). 17

Figure 6. ORTEP drawings of 2,2'-*bis*(2-cyanato)-1,1'-naphthyl) (**4**) , 1,2-*E*-*bis*(4-cyanato-3-methoxyphenyl)ethene (**7**), and, 1,2-*bis*(4-cyanato-3-methoxyphenyl)ethane (**8**) taken from the single-crystal x-ray diffraction molecular-structure determinations 20

Figure 7. TGA/FTIR analysis of compound **2**. 22

Figure 8. DSC data for various initial and post curing cycles of monomer **3** 23

Figure 9. TMA analysis after curing of vanillin bis(cyanate) ester monomer **8** 25

Figure 10. TGA/FTIR plot for the thermal heating of monomer **8**. Inset is the FT-IR spectra of the gases produced at the labeled temperature. The initial weight loss is due to residual THF in the sample of **8** 26

Figure 11. DSC scan of uncured **10** 28

Figure 12. DSC scan of uncured **11** 29

Figure 13. Residual cure of **11** as measured by DSC 30

Figure 14. Oscillatory TMA scan of cured **10** (dry) 30

Figure 15. Oscillatory TMA scan of **10** after exposure to 85 °C water for 96 h 31

Figure 16. Oscillatory TMA of cured **11** (dry) 32

Figure 17. Oscillatory TMA of cured **11** after exposure to 85 °C water for 96 h 33

Figure 18. DSC scan of compound **12** 33

Figure 19. Picture of composite flat panels prepared from compound **12** 34

Figure 20. ORTEP of compound 18 and composite photograph of the crystalline product.....36

Figure 21. DSC scan of compound **18** 37

List of Schemes

Scheme 1. Isolation of natural vanillin.....5

Scheme 2. Conversion of guaiacol and catechol to vanillin.....5

Scheme 3. Conversion of vanillin to (**2**).....18

Scheme 4. Synthesis of (**3**) and (**4**).....19

Scheme 5. Reductive coupling of vanillin to produce bis-phenols and ultimately cyanate esters (**7**) and (**8**) 19

Scheme 6. Proposed mechanism for the decomposition of methoxy-functionalized cyanate esters 22

Scheme 7. Decomposition mechanisms for cured cyanate esters at elevated temperature 23

Scheme 8. General synthesis of single-ring *bis*-cyanate esters from phloroglucinol.....27

Scheme 9. Synthesis of single-ring *bis*-cyanate esters studied in theis work.....27

Scheme 10. Synthesis of a tricyanate ester from 1-(chloromethyl)-4-methoxybenzaldehyde.....35

List of Tables

Table 1. Selected crystallographic data and structure refinement parameters for **4**, **7**, and **8**.....20

List of Symbols, Abbreviations, and Acronyms

NAWCWD	Naval Air Warfare Center, Weapons Division
NMR	Nuclear Magnetic Resonance
IR	Infrared (spectroscopy)
FTIR	Fourier Transform Infrared (spectroscopy)
ATR-FTIR	Attenuated Total Reflectance Fourier Transform Infrared (spectroscopy)
DSC	Differential Scanning Calorimetry
TGA	Thermal Gravimetric Analysis
TMA	Thermomechanical Analysis
DoD	Department of Defense
T_g	Glass Transition Temperature
DMF	Dimethyl Formamide
THF	Tetrahydrofuran
CNBr	Cyanogen Bromide
TEA	Triethylamine
NDGA	Nordihydroguarietic Acid
DMSO	Dimethylsulfoxide
OTMA	Oscillatory Thermomechanical Analysis
AFRL-RZ	Air Force Research Laboratory, Propulsion Directorate
mp	Melting Point
mL	Milliliter
KO*t*Bu	Potassium *tert*-Butoxide
MeCN	Acetonitrile
ORTEP	Oak Ridge Thermal Ellipsoid Plot Program
LECy	*bis*-Cyanate Ester Prepared from 4,4'-(ethane-1,1-diyl)diphenol
MeOCN	Methyl *iso*-Cyanate
ppm	Parts Per Million (concentration)
SiMCy	*bis*-Cyanate Ester Prepared from 4,4'-(dimethylsilanediyl)diphenol
HOAc	Acetic Acid
EtOH	Ethanol

Acknowlegements

The authors would like to thank the SERDP Weapons and Platforms Office, under the direction of Mr. Bruce Sartwell, for providing funding and administrative support that allowed for this project to proceed. We would also like to thank Drs. Stephen Fallis and Robin Nissan for their local managerial support. This project was initially proposed and funded under another PI, Dr. Andrew Guenthner, and the authors are indebted to him not only for his foresight in proposing such innovative research, but also his technical expertise and willingness to collaborate with NAWCWD after his move to the AFRL propulsion directorate. Special thanks go to Dr. Michael Wright for his efforts in helping to guide this research and composing large sections of this report. Technical support for this project was provided by a number of talented NAWCWD scientists including Mr. Scott Compel and Dr. Matthew Davis (synthesis of cyanate ester resins), Dr. Lee Cambrea (IR, TGA/IR experiments), Dr. Heather Meylemans and Mr. Sean McCormick (synthesis of cyanate ester resins), Dr. Thomas Groshens (single crystal X-ray diffraction experiments), Dr. Lawrence Baldwin (thermal analysis), Mr. Mike Ford, Ms. Shannon Haines, and Ms. Jessica Cash (synthesis of cyanate ester resins, creosote bush extraction). Lastly, the authors would like to thank Mr. Kevin Lamison (composite fabrication).

1. Abstract

Objectives: Demonstrate the feasibility of converting diaryl or single-ring polyphenols that are extracted or derived from sustainable and renewable plant sources to cyanate ester resins for use in high-performance polymer composites.

Technical Approach: Cyanate esters were prepared from several different renewable sources including mixed extracts from creosote bush leaves and stems, diaryl *bis*-phenols derived from both the oxidative and reductive coupling of vanillin, resveratrol, and single-ring systems derived from resorcylic acid. These resins were fully characterized by techniques including NMR and IR spectroscopy, mass spectrometry, and in some cases, single crystal X-ray diffraction. The resins were further characterized by thermal analysis utilizing techniques including DSC, TGA, and TMA. The thermal stability and decomposition of resins was monitored with TGA/IR experiments.

Results: Several new extraction procedures were developed to isolate polyphenols from the leaves and stems of the creosote bush. These crude mixtures could be converted to cyanate esters, but upon work-up the mixtures rapidly polymerized, even at room temperature and this system was not studied further. Three synthetic routes were then pursued to evaluate the best route to high performance, renewable cyanate esters. In the first route, vanillin was successfully coupled by both an oxidative and a reductive route to produce two biaryl structures. These *bis*-phenols were then cyanated and fully characterized. The reductively coupled vanillin structure underwent complete cure and the thermomechanical properties of the polymer were assessed. A T_g of 202 °C was observed by TMA (tan δ). The thermal stability of the vanillin derived resins was also evaluated with TGA/IR experiments. Both resins showed good thermal stability up to ca. 310 °C and then decomposed with evolution of methyl isocyanate. This novel decomposition pathway results from decomposition of the cyanurate ring in conjunction with the ortho-methoxy groups of the aromatic rings, but does not affect the use temperature of these materials as the decomposition proceeds at a temperature far beyond the glass transition temperature. In the second synthetic route, 3,5-dihydroxybenzoic acid was functionalized with different alkyl groups and several new cyanate esters were prepared. The T_g was found to decrease with increasing alkyl chain length. The T_g of the methyl derivative was determined to be 315 °C, while for R = ethylhexyl the T_g dropped to 150 °C. Water uptake in these resins was inversely proportional to chain length. The propyl derivative was produced on a multigram scale and glass fiber composite flat panels were successfully fabricated. In the final route, resveratrol was hydrogenated and converted to a tricyanate ester. The resin melts at 120 °C and on the basis of DSC data is shown to cure completely.

Benefits: The highly efficient and environmentally favorable synthetic procedures developed through this research will allow for the use of renewable cyanate esters that address the demanding requirements of the warfighter. In addition to reducing net carbon emissions by utilizing renewable carbon as the feedstock for these materials, use of the methods developed through this program have the potential to greatly reduce solvent use and the overall energy footprint of production and fabrication processes.

2. Objective

Composite materials consisting of an organic resin and fiber support are widely used throughout the DoD and the adoption of these materials in place of metal and ceramic components is accelerating. Composites provide a number of performance advantages over conventional materials including a significant reduction in weight leading to reduced fuel usage and greater range for tactical vehicles, particularly aircraft. Although increased use of composites provides several environmental advantages, these benefits are offset by the non-sustainable derivation of resins from petroleum products. To address this shortcoming, this project is focused on the efficient synthesis of high performance cyanate ester resins from sustainable and renewable polyphenols utilizing methods with low environmental impact.

The ultimate goal of this project is to demonstrate the suitability of renewable cyanate ester resins for use in high performance composites. Successful completion of this goal will allow for enough risk reduction to warrant transition of this work to a full SERDP program. Specific goals of the project include the following: 1) Discovery of optimal conditions for the efficient and environmentally favorable extraction of polyphenols from the leaves and stems of the creosote bush (Larrea tridentate). 2) Conversion of extracted polyphenols to a mixture of cyanate esters. 3) Evaluation of mixed cyanate esters derived from creosote bush extract as a resin system for the assembly of high performance thermosets. 4) Development of methods for the efficient coupling of vanillin and vanillin derivatives to produce bis-phenols and subsequent cyanate esters. 5) Synthesis of resorcylic acid esters and subsequent *bis*-cyanate esters from α-resorcylic acid. 6) Synthesis of a tricyanate ester from hydrogenated resveratrol. 7) Complete characterization of all new materials utilizing a suite of analytical techniques. 8) Evaluation of the cure chemistry of renewable cyanate esters to include a) determination of the degree of cure, b) characterization of potential off-gassing during cure, c) determination of the ability of a particular resin to yield a void free thermoset. 9) Evaluation of the thermomechanical properties (glass transition temperature, decomposition temperature) of robust thermoset structures resulting from cross-linked cyanate ester resins. 10) Fabrication of flat panel test articles to demonstrate the suitability of renewable cyanate esters for the production of composite parts.

3. Background

Although epoxy resins are widely used in composites for DoD applications, they suffer from a number of disadvantages that have both limited the adoption of lightweight polymer-based composites and drive the search for effective replacement materials.[1] A number of candidate replacement materials with superior properties, such as cyanate ester resins and polyimide resins have been identified and tested. Large-scale adoption of these resins, however, has been significantly slowed by the high costs associated with completing the DoD materials qualification process which demands a large program of testing and verification of properties. Since any new composite resin based on renewable sources (including any epoxy resin derived from natural products) will also require qualification, a higher payoff (through higher risk) approach would be to develop and qualify a renewable "next generation" composite resin. Qualification and fielding efforts would then yield not only the advantages of using sustainable and renewable resources, but also the superior performance, lower costs, and improved reliability associated with "next generation" composite resins. The availability of these resins will provide a more compelling case for replacing heavier metal and ceramic structures, particularly in aerospace applications, where the associated fuel savings and gains in performance are most visible and dramatic.

Cyanate ester resins represent a particularly attractive class of materials for new Navy and DoD applications due to their superior physical properties and ease of processing, which are available at total productions costs similar to high-performance epoxy resins. At present, cyanate esters are mainly used in radomes and (as blends with epoxy resins) in circuit boards, as well as in structures for space satellites.[2] Additional potential applications under investigation include airframes for weapons, helicopters, parts near aircraft engines, and in marine infrastructure. Cyanate esters offer significant advantages over epoxy resins in maximum use temperature (often 400 °F or higher), fire resistance (which is becoming a major concern on commercial aircraft), warm or cold stability in wet environments, and dimensional stability. Cyanate esters exhibit low toxicity, are non-irritating, and do not require separate additives for curing.[3] The curative agents required for high-performance epoxy resins are often significantly more hazardous than the resin itself, and would likely remain a significant hazard for epoxy resins based on renewable resources.

There are two major classes of commercial cyanate ester resins: diaryl (or "bisphenol type") cyanate esters based on derivatives of bisphenol A and similar molecules that feature an aromatic ring at either end with more flexible intervening chemical linkages (Figure 1), and mono- or tri-aryl "novolac type" cyanate esters that feature a higher density of cyanate ester linkages and aromatic rings separated by little or no intervening flexible bonds. Among the "novolac type" cyanate esters, the triaryl monomers are strongly preferred for widespread utilization. Although they exhibit higher maximum use temperatures, they tend to suffer from brittleness and an inability to dissolve thermoplastic toughenners compared to "bisphenol type" cyanate esters. Unless prepolymerized, they tend to be solids at room temperature.[3] The "bisphenol type" cyanate esters are not only inherently tougher, they also typically can dissolve 20% by weight or more of thermoplastic toughenners (such as polycarbonates) that render them much more robust in practical use situations without sacrificing maximum use temperatures. Interestingly, many naturally available phytochemicals are diaryl compounds similar to

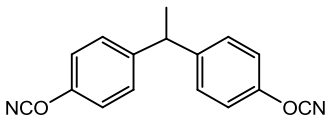

LeCy

Figure 1. Typical petroleum-based dicyanate ester monomer

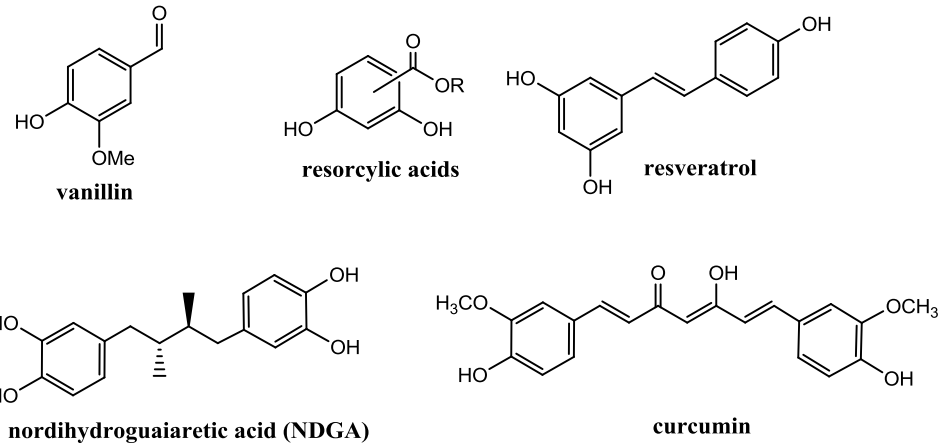

Figure 2. Selected structures of naturally occuring phenolics examined in this work

bisphenol A. Unlike their synthetic counterparts, these compounds often confer significant potential health benefits as antioxidants.

Several naturally occurring bis-phenols and precursors can be readily extracted from plants. For example, a major component of the creosote bush (Larrea tridentate) which dominates the arid landscapes of the Mojave, Sonoran, and Chihuahuan Deserts of North America is an excellent source of polyphenolic compounds which make up several weight % of the leaves roots and stems of the plant. The most prevalent of these bis-phenols is nordihydroguaiaretic acid (NDGA). Other promising polyphenols are resveratrol, a well-known antioxidant found in grape skins and extracted from Japanese Knotweed, and curcumin which is found in turmeric (Figure 2).

An alternative approach is to build bis-phenols from readily available and easily extracted renewable chemicals such as vanillin. One current method of production of vanillin involves isolation from the seed pods of the orchid *vanillin planifola.*[4] *V*anillin represents ~2 % of the dry weight of the seed pods. Vanillin is chemically bound in the seeds as the β-D-glycoside and after a drying and aging period, the pure vanillin is released and isolated (Scheme 1).[4] Of the ~6000 tons of vanillin used per year, this isolation process from plants accounts for only ~0.2% of the world's consumption.[5]

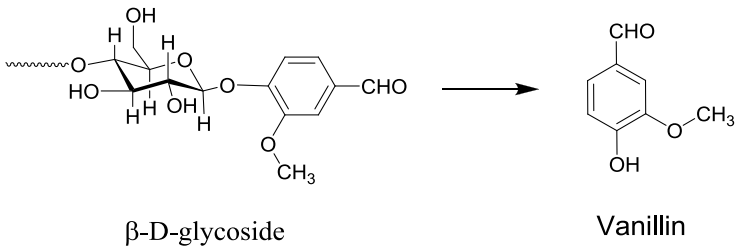

Scheme 1. Isolation of natural vanillin

One significant route to synthetic vanillin currently begins with guaiacol.[6] Guaiacol can be isolated from the plant *guaiacum*; however, based on feedstock and isolation costs, the guaiacol is currently prepared from petroleum derived catechol (Scheme 2).[7] Thus, this later route from catechol represents a non-renewable source of vanillin. The third method that is currently used to produce vanillin is based on the biofeedstock lignin.[8] Lignin is the second most abundant organic polymer on the planet (Figure 3). On a commercial scale, lignin can be depolymerized with base under oxidative-conditions to form vanillin in reasonable yield and in a cost effective manner.[9] In the 1980's, lignin waste from one paper mill was the source for ~60% of the world's vanillin supply. More recently, lignin has become a useful by-product of cellulosic biofuel production.[10] Lignin is at present the most viable and cost effective source of renewable bioaromatics. As a consequence, new methods for both improving chemical

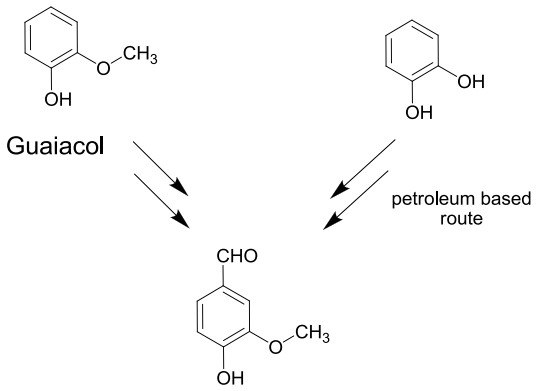

Scheme 2. Conversion of guaiacol and catechol to vanillin

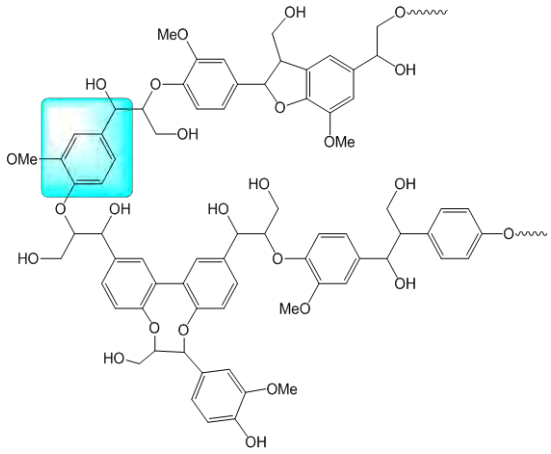

Figure 3. Graphical depiction of lignin

efficiencies and also reducing the waste stream associated with isolating well defined monomeric/dimeric aromatic structures from lignin are under continual development.[11]

A third option that presents itself is the use of advanced bioengineering techniques that result in the selective production of phenols suitable for conversion to high performance resins. One key starting material is phloroglucinol that can be readily converted to resorcinol and subsequently resorcyclic acids. These acids are incredibly useful materials for the synthesis of cyanate ester resins with tunable properties including T_g, water uptake, toughness, stiffness, and thermal stability.

Polyphenolic compounds may be readily converted to cyanate ester resins through reaction with cyanogen bromide at temperatures just below room temperature in the presence of a base such as triethylamine. The reaction typically generates quantitative conversion of phenols to cyanate esters (which may be liquid at room temperature or solids with low melting points). The cyanate ester resins can then be melted (if needed), mixed with reinforcing fibers, and thermally cured at temperatures ranging from room temperature to 550 °F to fabricate useful structures. Although recycling of the finished products is more difficult than recycling thermoplastics, a number of potential environmentally-friendly recycling methods are in development for thermosets such as cyanate esters that have reached the end of service.[12]

4. Materials and Methods

4.1 Chemical Synthesis

4.1.1 General methods. All manipulations of compounds and solvents were carried out using standard Schlenk techniques. ^{1}H and ^{13}C NMR measurements were performed using a Bruker AC 200 or Bruker 400 MHz instrument. ^{1}H and ^{13}C NMR chemical shifts are reported versus the deuterated solvent peak (Solvent: ^{1}H, ^{13}C: $CDCl_3$, δ 7.25 ppm, δ 77.0 ppm). Anhydrous dimethylformamide (DMF), inhibitor free anhydrous tetrahydrofuran (THF), inhibitor free anhydrous diethyl ether, vanillin, platinum oxide (PtO_2), titanium tetrachloride, 2-methoxy-4-methylphenol, methyltributylamonium chloride (aq. 70 wt-%), anhydrous triethyl amine, and cyanogen bromide were purchased from Aldrich Chemical Co. and used as received. Elemental analyses were performed at Atlantic Microlab, Inc., Norcross, GA. DSC measurements were performed using either a TA Instruments Q100 or Q200 differential scanning calorimeter under a N_2 purge of 30 cc/min and 30 cc/min, respectively.

4.1.2 Chloroform extraction of creosote leaves and stems. 24 g of leaves and stems from a locally grown creosote bush (*Larrea tridentata*) specimen were boiled in 450 mL of chloroform for about 7 minutes. The yellow solution was filtered and the solvent removed under reduced pressure to yield 1.5 g of yellow powder. A 25 mL round-bottomed flask equipped with magnetic stirbar was charged with 430 mg of the creosote extract and 10 mL acetone. The mixture was stirred in an ice bath. In one portion, 660 mg CNBr was added and allowed to completely dissolve. Then, 580 mg triethylamine (TEA) was added dropwise and a white solid (TEA/HCl salt) precipitated shortly thereafter. After stirring for 30 min, the solid was filtered and the solvent was removed under reduced pressure (ambient, 10 torr) leaving a pale yellow, viscous oil.

4.1.3 Isolation of NDGA from creosote leaves and stems. To a one liter round bottom flask were added 25 g of creosote leaves and stems and 650mL of an aqueous solution that was 5% NaOH and 2.5% sodium hydrosulfite. The mixture was then sonicated for 30 minutes. The organic matter was removed by filtration to give a dark brown solution which was acidified to a pH of about 5 by litmus paper test using concentrated hydrochloric acid. A yellow precipitate formed, and was allowed to settle out before proceeding. The water was then decanted off, leaving behind a brown sludge, which was dissolved in 50 mL of methanol. The solution was diluted with 250 mL of diethyl ether and a large mass of powdery solid precipitated and was collected. The ether solution was washed with 250 mL of water and then extracted with ten 4mL portions of the 5% NaOH/2.5% $Na_2S_2O_4$. These different fractions produced varying amounts of NDGA upon acidification, but most of it was contained in fractions 2-6. The product was washed with cold glacial acetic acid or recrystallized from 36% aqueous acetic acid to produce pure NDGA

4.1.4 Preparation of a cyanate ester from NDGA. A mixture of 100 mg NDGA and 157 mg cyanogen bromide (4.5 equiv) in 5 mL anhydrous acetone was cooled and stirred in an ice bath. Over 5 min, 133 mg of triethylamine (4 equiv) was added dropwise. Shortly thereafter, a white precipitate of triethylamine hydrogen bromide formed. After 1 h, the mixture was

filtered. The solvent was rotary evaporated (bath temperature 30 °C) to leave a colorless residue that was insoluble in all common organic solvents.

4.1.5 Preparation of 3,3'-dimethoxy-5,5'-dimethyl-[1,1'-biphenyl]-2,2'-diol (1). $Bu_3MeNMnO_4$ (10.9 g, 34.1 mmol) was dissolved in CH_2Cl_2 (250 mL) placed in an ice bath and allowed to cool. Then 2-methoxy-4-methylphenol (9.95 g, 72.0 mmol) was added dropwise to the CH_2Cl_2 solution and allowed to react with stirring for 1 h at 0 ºC under N_2. The reaction mixture was diluted with H_2O (~200 mL) and the mixture stirred for an additional 30 min. The mixture was filtered through a glass-wool plug to remove the MnO_2 and the organic layer separated. The organic layer was washed with 0.1 M HCl (3 x 150 mL), brine (50 mL), and then dried over $MgSO_4$. Removal of the solvent under reduced pressure afforded **1** as a yellow powder (5.97 g, 60% yield). Purification of **1** was achieved using column chromatography on silica gel and elution with ethyl acetate/hexanes (1/4, v/v) to afford a 50% overall yield.

4.1.6 Preparation of 2,2'-dicyanato-3,3'-dimethoxy-5,5'-dimethyl-1,1'-biphenyl (2). A THF (30 mL) solution containing **1** (0.971 g, 3.5 mmol) and CNBr (1.032 g, 9.8 mmol) was placed in a dry ice and acetone bath at -40 ºC. Et_3N (0.738 g, 7.30 mmol) was added and the solution was allowed to stir at -40 ºC for 2 h under N_2. The solution was diluted with ether (~150 mL) and washed with water (2 x 200 mL), brine (50 mL), and then dried over $MgSO_4$. Removal of the solvent under reduced pressure afforded **2** as an off-white powder (1.06 g, 94%). Further purification can be achieved by recrystallization from acetonitrile (0.96 g, 85%). ^{1}H NMR ($CDCl_3$) δ 6.91 (d, J = 2 Hz, 2 H), 6.72 (d, J = 2 Hz, 2H), 4.00 (s, 3H) 2.41 (s, 3H); ^{13}C NMR ($CDCl_3$) δ 150.1, 138.9, 137.8, 127.2, 123.1, 114.5, 110.2, 56.7, 21.7. Anal. Calcd for $C_{18}H_{16}O_4N_2$: C, 66.86; H, 4.97. Found: C, 65.77; H 5.09.

4.1.7 Preparation of 2,2'-bis(cyanato)-1,1'-biphenyl (3). Using the procedure above monomer **3** was prepared in 65% yield: ^{1}H NMR ($CDCl_3$) δ 7.64 (dd, J = 8, 1.5 Hz, 2 H), 7.59 (psuedo dt, J = 8, 2 Hz, 2H), 7.45 (psuedo dt, J = 8, 2 Hz, 2H), 7.38 (dd, J = 8, 2 Hz); ^{13}C NMR ($CDCl_3$) δ 150.2 (ipso-OCN), 132.5, 131.1, 127.4, 124.2, 115.3, 108.4. Anal. Calcd for $C_{14}H_8O_2N_2$: C, 71.18; H, 3.42. Found: C, 71.28; H 3.46.

4.1.8 Preparation of 2,2'-bis(cyanato)-1,1'-binaphthyl (4). Using the procedure above monomer **4** was prepared in 65% yield: ^{1}H NMR ($CDCl_3$) δ 8.22 (d, J = 9 Hz, 2 H), 8.05 (d, J = 8 Hz, 2H), 7.88 (d, J = 9 Hz, 2 H), 7.60 (ddd, J = 8, 7, 1 Hz, 2H), 7.45 (ddd, J = 8, 7, 1 Hz, 2 H), 7.17 (dd, J = 8, 1 Hz, 2H); ^{13}C NMR matched that reported in the literature.[13]

4.1.9 Preparation of (*E*)-4,4'-(ethene-1,2-diyl)bis(2-methoxyphenol) (5). A flask was charged with 2.35 g of Mg (96.7 mmol) and anhydrous THF (100 mL). The mixture was chilled to -78 °C and then $TiCl_4$ (10.6 mL, 96.5 mmol) was added dropwise through an addition funnel. The flask was allowed to slowly warm up to room temperature and the mixture transitioned to a green slurry and finally a black solution. After stirring at room temperature for 30 min a THF (50 mL) solution of vanillin (7.01 g, 46.1 mmol) was added dropwise. The reaction was mildly exothermic and resulted in a dark brown mixture. The mixture was heated at reflux for 16 h and was then cooled to room temperature. The solvent was removed under reduced pressure and the residue treated with 100 mL of 2 M HCl to yield a dark solution with pale brown suspended solid. The mixture was filtered on a medium frit and the isolated solid was washed with water (3

x 50 mL) and chilled ethanol (3 x 25 mL 0 °C). The solid was dried in a vacuum oven (~10 Torr, 45 °C) overnight to yield 2.91 g of pale brown solid (46% yield). The purity of the crude product (>98%) was suitable for later synthetic procedures, but the material can be further purified by dissolution in THF followed by precipitation with hexane. X-ray quality crystals were grown by slow evaporation of a concentrated THF solution. ^{1}H NMR (dimethylsulfoxide (DMSO)-d_6): δ 9.07 (s, 2H, Ph-OH), 7.13 (d, 2H, J = 2 Hz), 6.94 (s, 2H), 6.93 (dd, 2H, J = 8, 2 Hz), 6.73 (d, 2H, J = 8 Hz), 3.81 (s, 6H, OMe); ^{13}C NMR (DMSO-d_6): δ 147.8, 146.2, 129.2, 125.8, 119.5, 115.6, 99.6, 55.6.

4.1.10 Preparation of 4,4'-(ethane-1,2-diyl)bis(2-methoxyphenol) (6). A Parr reaction vessel was charged with (*E*)-4,4'-(ethene-1,2-diyl)bis(2-methoxyphenol) (2.85 g, 10.5 mmol), THF (50 mL), PtO_2 (70 mg), and then placed under hydrogen (30 psig) and allowed to react at ambient temperature for 16 h with continuous agitation. The mixture was filtered through glass wool to remove platinum and the THF was removed under reduced pressure. The solid was washed with hexanes (2 x 30 mL) and dried under reduced pressure to afford 2.62 g of light brown solid (91% yield). ^{1}H NMR (DMSO-d_6) δ 8.66 (s, 2H, Ph-OH), 6.73 (s, 2H), 6.65-6.53 (m, 4H), 3.70 (s, 6H, OMe), 2.70 (s, 4H, CH_2); ^{13}C NMR (DMSO-d_6): δ 147.7, 144.9, 133.1, 120.9, 115.6, 113.1, 56.0 (OMe), 37.6 (CH_2).

4.1.11 Preparation of (*E*)-1,2-bis(4-cyanato-3-methoxyphenyl)ethene (7). A round bottom flask was charged with 0.70 g (2.6 mmol) of (*E*)-4,4'-(ethene-1,2-diyl)bis(2-methoxyphenol), THF (30 mL), and CNBr (0.69 g, 6.5 mmol). The mixture was chilled to -78 °C and triethylamine (0.75 mL) was then added dropwise by syringe. The pale brown solution was allowed to warm to room temperature and a tan solid precipitated. After stirring at ambient temperature for 20 min, the slurry was filtered and solid collected on a medium glass-frit. The solid was washed with water (3 x 20 mL) and air dried to yield 640 mg (77%) of the crude product. Recrystallization from hot THF yielded 530 mg of off-white needles. Crystals suitable for an X-ray diffraction study were grown by slowly cooling a concentrated acetonitrile solution. ^{1}H NMR (DMF-d_7) δ 7.66 (d, 2H, J = 2 Hz), 7.60 (d, 2H, J = 9 Hz), 7.50 (s, 2H, -CH=CH-), 7.35 (dd, 2H, J = 9, 2 Hz), 4.07 (s, 3H, OMe)

4.1.12 Preparation of 1,2-bis(4-cyanato-3-methoxyphenyl)ethane (8). A round bottom flask was charged with 1.05 g (3.8 mmol) of 4,4'-(ethane-1,2-diyl)bis(2-methoxyphenol), THF (40 mL), and of CNBr (1.06 g, 10 mmol). The flask was cooled to -20 °C and triethylamine (1.16 mL) was added dropwise. A tan solid immediately precipitated from solution. The mixture was stirred at -20 °C for 10 min and was then removed from the cold bath and allowed to spontaneously warm. After stirring for an additional 30 min, the mixture was filtered on a medium glass-frit and the solid washed with water (3 x 20 mL) and then air dried to yield 0.71 g of crude product. Evaporation of the filtrate followed by water and ether washes yielded an additional 0.22 g of product for a total of 0.93 g (76%). Recrystallization from hot THF yielded 625 mg of tan needles. ^{1}H NMR (DMSO-d_6) δ 7.42 (d, 2H, J = 8 Hz), 7.18 (s, 2H), 6.91 (d, 2H, J = 8 Hz), 3.88 (s, 3H, OMe), 2.91 (s, 2H, CH_2). Anal. Calcd for $C_{18}H_{16}O_4N_2$: C, 66.86; H, 4.97. Found: C, 66.67; H 4.96.

4.1.13 Preparation of 5-(2-ethylhexyloxy)resorcinol (9). A DMF (50 mL) solution containing anhydrous phloroglucinol (5.00 g, 39.6 mmol) was treated with t-BuOK (5.61 g, 47.5 mmol, based on 95% purity)**.** After stirring at ambient temperature for 30 min the 2-ethylhexyl

bromide (8.42 mL, 47.5 mmol) and sodium iodide (0.50 g) were added in that order. The mixture was heated at ~50 ^{o}C for 24 h with stirring. The mixture was cooled to ambient temperature and diluted with ether (200 mL) and washed with water (4 x 200 mL), brine (100 mL), and then the organic layer was dried over magnesium sulfate. The drying agent was removed by filtration and the solvents removed under reduced pressure. The crude product was subjected to column chromatography on silica gel. Elution with hexanes/ethyl acetate (4/1, v/v) afforded pure 5-(2-ethylhexyloxy) resorcinol (2.00 g, 20 %) as light yellow oil after solvent removal. ^{1}H NMR ($CDCl_3$) δ 5.99 (brs, aromatic CH, 3 H), 3.72 (d, J = 6 Hz, OCH_2), 1.65 (apparent septant, 1 H), 1.3-1.5 (overlapping multiplets, CH_2's, 8 H), 0.87 (t, J = 7.4 Hz, CH_3's, 6 H).

4.1.14 Preparation of 5-(2-ethylhexyloxy)-1, 3-*bis*(cyanato)benzene (10). A chilled (-20 ^{o}C) diethyl ether solution (60 mL) containing **9** (1.64 g, 6.9 mmol) and cyanogen bromide (1.82 g, 17 mmol) was treated with triethylamine (1.77 mL) via dropwise addition. The resulting mixture was stirred for 30 min and then filtered through a pad of Celite. The Celite was washed with ether (40 mL) and the organic layer was washed with water (2 x 150 mL), brine (100 mL), and then dried over magnesium sulfate. The drying agent was filtered off and the solvent removed under reduced pressure to afford 1.78 g (86%) of the bis(cyanate) ester as a light amber oil. ^{1}H NMR ($CDCl_3$) δ 6.81 (d, J= 2 Hz, 2H), 6.78 (t, J= 2 Hz, 1 H), 3.86 (d, J = 6 Hz, OCH_2), 1.72 (apparent septant, 1 H), 1.3-1.5 (overlapping multiplets, CH_2's, 8 H), 0.90 (t, J = 7.4 Hz, CH_3, 3 H), 0.88 (t, J = 7.4 Hz, CH_3, 3 H). ^{13}C NMR ($CDCl_3$) δ 162.2 (aromatic ipso -OCH_2), 154.0 (aromatic ipso -OCN), 107.5 (OCN), 100.4 (aromatic CH, *C4* & *C6*), 72.0 (OCH_2), 39.1 (CH), 30.3, 28.9, 23.7, 22.9 (CH_2's), 13.9, 11.0 (CH_3's).

4.1.15 Preparation of methyl-3,5-*bis*(cyanato)benzoate (11). A chilled (-20 ^{o}C) diethyl ether solution (100 mL) containing methyl 3,5-dihydroxybenzoate (3.00 g, 17.8 mmol) and cyanogen bromide (4.70 g, 44.4 mmol) was treated with triethylamine (5.2 mL) via dropwise addition. The resulting mixture was stirred for 1 h, diluted with ether (100 mL), and the organic layer was washed with water (3 x 250 mL), brine (100 mL), and then dried over magnesium sulfate. The drying agent was filter off and the solvent removed under reduced pressure to afford 3.30 g (85%) of methyl 3,5-bis(cyanate)benzoate an off white solid. ^{1}H NMR ($CDCl_3$) δ 7.93 (d, J= 2 Hz, 2H), 7.43 (t, J= 2 Hz, 1 H), 3.95 (s, OCH_3, 3H); ^{13}C NMR ($CDCl_3$) δ 163.1 (CO_2), 153.1 (aromatic ipso -OCN), 135.0 (aromatic C), 114.7 (aromatic CH), 108.1 (OCN), 107.0 (aromatic CH), 53.2 (OCH_3).

4.1.16 Preparation of propyl-3,5-*bis*(cyanato)benzoate (12). A chilled (-20 ^{o}C) diethyl ether solution (200 mL) containing propyl 3,5-dihydroxybenzoate (5.00 g, 25.5 mmol) and cyanogen bromide (7.95 g, 75.1 mmol) was treated with triethylamine (8.0 mL) via dropwise addition. The resulting mixture was stirred for an additional 1 h at -20 ^{o}C, diluted with ether (100 mL), and the organic layer was washed with water (3 x 250 mL), brine (100 mL), and then dried over magnesium sulfate. The drying agent was filter off and the solvent removed under reduced pressure to afford 5.30 g (85%) of propyl 3,5-bis(cyanate)benzoate as a white solid (DSC m.p. 69-70 ^{o}C). ^{1}H NMR ($CDCl_3$) δ 7.96 (d, J= 2 Hz, 2H), 7.44 (t, J= 2 Hz, 1 H), 4.34 (d, J = 7 Hz, OCH_2, 2H), 1.80(dt, J = 7 Hz, CH_2, 2H), 1.01 (t, J = 7 Hz, CH_3, 3H); ^{13}C NMR ($CDCl_3$) δ 162.7 (CO_2), 153.2 (aromatic ipso -OCN), 135.6 (aromatic C), 114.7 (aromatic CH), 107.9 (OCN), 107.1 (aromatic CH), 68.1 (OCH_2), 21.9 (CH_2), 10.3 (CH_3).

4.1.17 Preparation of (*E*)-3,4',5-tricyanatostilbene (13). A 20 mL round-bottomed flask equipped with magnetic stirring bar was charged with 100 mg of trans-resveratrol (0.4 mmol), 186 mg CNBr (1.7 mmol, 4 equiv) and 10 mL anhydrous acetone. The mixture was stirred in a -20 °C bath before 133 mg TEA (1.3 mmol, 3 equiv) was added dropwise. After stirring 2 h, the reaction mixture was diluted with 20 mL H_2O. The crude white product was collected on a medium porosity glass frit and dried under vacuum. Recrystallization from EtOH gave the title compound as colorless needles. mp 161-163 °C. δ_H ($CDCl_3$): 7.63 (d, J = 8.7 Hz, 2H), 7.44 (d, J = 2.4 Hz, 2H), 7.36 (d, J = 8.9 Hz, 2H), 7.22 (d, J_{AB} = 16.4 Hz, 1H), 7.14 (t, J = 2.4 Hz, 1H), 7.05 (d, J_{AB} = 16.3 Hz, 1H); δ_C ($CDCl_3$): 153.93, 153.21, 142.41, 134.71, 132.17, 129.27, 126.34, 116.26, 111.33, 108.59, 107.72, 103.29. Elemental analysis calculated for $C_{17}H_9N_3O_3$: C, 67.33; H, 2.99; N, 13.86. Found: C, 67.33; H, 2.86; N, 13.92.

4.1.18 Preparation of diethyl-4-methoxybenzylphosphonate (14). A 100 mL round-bottomed flask equipped with magnetic stirring bar and reflux condenser was charged with 15.6 g of 4-methoxybenzyl chloride (100 mmol) and 16.6 g triethylphosphite (1 equiv). The mixture was heated to 120 °C for 5 h. Reduced pressure distillation gave 24.46 g of the title compound as a colorless oil (94 %). δ_H ($CDCl_3$): 7.23 (dd, J = 9.0 and 2.2 Hz, 2H), 6.86 (d, J = 8.2 Hz, 2H), 4.02 (pent, J = 7.2 Hz, 4H), 3.81 (s, 3H), 3.10 (d, $^2J_{PCH}$ = 21.1 Hz, 2H), 1.26 (t, J = 7.2 Hz, 6H); δ_C ($CDCl_3$): 158.82, 130.94 (d, J_{PC2} = 6.5 Hz), 123.69 (d, J_{PC1} = 9.4 Hz), 114.21 (d, J_{PC3} = 2.7 Hz), 62.23 (d, J_{POC} = 6.5), 55.43, 33.02 (d, J_{PC} = 139.6 Hz), 16.58 (d, J_{POCC} = 6.1 Hz). Elemental analysis calculated for $C_{12}H_{19}O_4P$: C, 55.81; H, 7.42. Found: C, 55.81; H, 7.46.

4.1.19 Preparation of (*E*)-3,4',5-trimethoxystilbene (15). A 1 L round-bottomed flask equipped with a magnetic stirring bar and reflux condenser was charged with 18.62 g of **14** (72 mmol, 1.2 equiv) and 500 mL anhydrous THF. In one portion, 8.74 g KO*t*Bu (78 mmol, 1.3 equiv) was added and allowed to stir until all the solids dissolved. 3,5-dimethoxybenzaldehyde (10 g, 60 mmol) was added in one portion and the mixture was refluxed overnight. After cooling to ambient, 200 mL H_2O and 3 mL glacial HOAc were added. The organic phase was separated and washed with 200 mL saturated aqueous $NaHCO_3$ followed by 200 mL brine. The organic phase was dried over anhydrous $MgSO_4$ and rotary evaporated leaving 16 g of a pale yellow solid (100 %). Recrystallization of the crude from EtOH gave the title compound as colorless plates. mp 53-55 °C. δ_H ($CDCl_3$): 7.45 (d, J = 8.7 Hz, 2H), 7.05 (d, J = 16.4 Hz, 1H), 6.90 (d, J = 16.4 Hz, 1H), 6.89 (d, J = 8.7 Hz, 2H), 6.65 (d, J = 2.5 Hz, 2H), 6.38 (t, J = 2.2 Hz, 1H), 3.83 (s, 9H); δ_C ($CDCl_3$): 161.26, 159.68, 139.97, 130.23, 129.01, 128.04, 126.86, 114.41, 104.63, 99.92, 55.59, 55.56. Elemental analysis calculated for $C_{17}H_{18}O_3$: C, 75.53; H, 6.71. Found: C, 75.43; H, 6.63.

4.1.20 Preparation of 3,4',5-trimethoxydibenzyl (16). A mixture of 6.17 g **15** (23 mmol), 500 mg 5% Pd/C and 100 mL EtOH was hydrogenated (40 psi) on a Parr® shaker for 4 h. The mixture was filtered through diatomaceous earth and rotary evaporated leaving 6.2 g of the title compound as a colorless oil (100 %). No further purification was necessary. δ_H ($CDCl_3$): 7.09 (d, J = 8.5 Hz, 2H), 6.82 (d, J = 8.5 Hz, 2H), 6.34 (d, J = 2.2 Hz, 2H), 6.31 (t, J = 2.3 Hz, 1H), 3.78 (s, 3H), 3.76 (s, 6H), 2.84 (m, 4H); δ_C ($CDCl_3$): 160.96, 158.11, 144.48, 134.05, 129.55, 113.98, 106.77, 98.16, 55.46, 55.44, 38.67, 36.98. Elemental analysis calculated for $C_{17}H_{20}O_3$: C, 74.97; H, 7.40. Found: C, 74.69; H, 7.50.

4.1.21 Preparation of 3,4',5-trihydroxydibenzyl (17). Recrystallization from toluene/EtOAc or H_2O gave the title compound as colorless plates. mp 159-161 °C. δ_H ($CDCl_3$/DMSO): 8.39 (s, 1 OH), 8.34 (2 OH), 6.99 (d, J = 8.4 Hz, 2H), 6.74 (d, J = 8.4 Hz, 2H), 6.23-6.18 (m, 3H), 2.8-2.62 (m, 4H); δ_C ($CDCl_3$/DMSO): 157.95, 155.00, 144.40, 132.95, 129.32, 115.38, 107.34, 100.75, 38.21, 36.67. Elemental analysis calculated for $C_{14}H_{14}O_3$: C, 73.03; H, 6.13. Found: C, 73.17; H, 6.14.

4.1.22 Preparation of 3,4',5-tricyanatodibenzyl (18). A procedure to similar to that used for **13** with 650 mg **17** (2.8 mmol), 1.17 g CNBr (11 mmol, 4 equiv), 860 mg TEA (8.4 mmol, 3 equiv) and 50 mL acetone. Obtained 760 mg of the product as a white solid (88 %). Recrystallization from heptane/EtOAc gave the title compound as long colorless needles. mp 118-120 °C. δ_H (DMSO): 7.47-7.39 (m, 5H), 7.39-7.33 (m, 2H), 3.04 (m, 2H), 2.94 (m, 2H); δ_H (DMSO): 152.67, 151.03, 147.51, 139.84, 130.75, 115.35, 114.31, 108.82, 107.92, 102.68, 36.18, 35.23. Elemental analysis calculated for $C_{17}H_{11}N_3O_3$: C, 66.88; H, 3.63; N, 13.76. Found: C, 66.86; H, 3.55; N, 13.66.

4.1.23 Preparation of (*E*)-4,4'-dicyanatostilbene (19). A procedure to similar to that used for **13** with 700 mg *E*-4,4'-(ethane-1,2-diyl)diphenol (3.3 mmol), 875 mg CNBr (8 mmol, 2.5 equiv) and 20 ml acetone. Recrystallization from MeCN gave the title compound as colorless plates. mp 173-175 °C. δ_H ($CDCl_3$): 7.58 (d, J = 9.0 Hz, 4H), 7.31 (d, J = 9.2 Hz, 4H), 7.06 (s, 2H); δ_C ($CDCl_3$): 152.50, 135.99, 128.63, 128.29, 115.97, 108.81. Elemental analysis calculated for $C_{16}H_{10}N_2O_2$: C, 73.27; H, 3.84; N, 10.68. Found: C, 73.26; H, 3.79; N, 10.86.

4.1.24 Preparation of 4,4'-dihydroxydibenzyl (20). A mixture of 3 g *E*-4,4'-(ethane-1,2-diyl)diphenol (14 mmol), 200 mg 5% Pd/C and 50 mL EtOH was hydrogenated (40 psi) on a Parr® shaker for 3 h. The mixture was filtered through diatomaceous earth and evaporated leaving a white solid. Recrystallization from HOAc gave 2.8 g of the title compound as colorless needles (95 %). mp 197-200 °C. δ_H ($CDCl_3$/DMSO): 8.45 (s, 2 OH), 6.98 (d, J = 8.4 Hz, 4H), 6.75 (d, J = 8.6 Hz, 4H), 2.77 (s, 4H); δ_C ($CDCl_3$/DMSO): 155.10, 132.55, 129.14, 115.16, 37.26. Elemental analysis calculated for $C_{14}H_{14}O_2 \cdot 0.1\ C_2H_4O_2$: C, 77.45; H, 6.54. Found: C, 77.86; H, 6.49.

4.1.25 Preparation of 4,4'-dicyanatodibenzyl (21). A procedure to similar to that used for **13** with 610 mg **20** (2.8 mmol), 750 mg CNBr and 20 mL acetone and cooled in a -20 C bath. Recrystallization of the crude solid from heptane to gave the title compound as colorless needles. mp 112-114 °C. δ_H ($CDCl_3$): 7.25-7.13 (m, 8H), 2.94 (s, 4H); δ_C ($CDCl_3$): 151.57, 139.95, 130.57, 115.49, 109.09, 36.96. Elemental analysis calculated for $C_{16}H_{12}N_2O_2$: C, 72.72; H, 4.58; N, 10.60. Found: C, 72.95; H, 4.54; N, 10.55.

4.1.26 Preparation of 4,4'-dihydroxydeoxybenzoin (22). A 250 mL round-bottomed flasked equipped with magnetic stirring bar and N_2 bubbler was charged with 7.55 g of 1,2-bis(4-methoxyphenyl)ethanone (29 mmol) and 27 g pyridine hydrochloride (232 mmol, 8 equiv). The mixture was heated in an oil bath at 190 °C for 8 h. The reaction was removed from the oil bath and carefully diluted with 100 mL H_2O. The tan precipitate (5.75 g, 87%) was collected on a coarse porosity glass frit. Recrystallization from H_2O gave the title compound as fine tan

needles. Mp 217-220 °C. δ_H (DMSO): 7.90 (d, J = 8.6 Hz, 2H), 7.04 (d, J = 8.6 Hz, 2H), 6.84 (d, J = 8.6 Hz, 2H), 6.68 (d, J = 8.6 Hz, 2H), 4.09 (s, 2H); δ_C (DMSO): 196.31, 162.01, 155.89, 131.05, 130.38, 127.94, 125.65, 115.26, 115.17, 43.49. Elemental analysis calculated for $C_{14}H_{12}O_3$: C, 73.67; H, 5.30. Found: C, 73.52; H, 5.22.

4.1.27 Preparation of 4,4'-dicyanatodeoxybenzoin (23). A procedure to similar to that used for **13** with 3.2 g **22** (14 mmol), 4.46 g CNBr (3 equiv), and 2.8 g TEA (2 equiv). Recrystallization from EtOH gave the title compound as colorless needles. mp 110-112 °C. δ_H ($CDCl_3$): 8.13 (d, J = 9.2 Hz, 2H), 7.44 (d, J = 9.2 Hz, 2H), 7.35 (d, J = 9.2 Hz, 2H), 7.30 (d, J = 9.2 Hz, 2H), 4.33 (s, 2H); δ_C ($CDCl_3$): 194.79, 155.92, 152.14, 135.11, 132.89, 131.82, 131.36, 115.93, 115.78, 108.81, 107.91, 44.55. Elemental analysis calculated for $C_{16}H_{10}N_2O_3$: C, 69.06; H, 3.62; N, 10.07. Found: C, 68.56; H, 3.64; N, 9.76.

4.1.28 Preparation of 1,3-dicyanato-5-(4-cyanatophenethyl)benzene (24). *trans*-Resveratrol was first hydrogenated under a 40 psi hydrogen atmosphere on a Parr shaker using THF as a solvent and 10% Pd/C as the catalyst (0.5 g catalyst/50 g resveratrol). The hydrogenated product, dihydroresveratrol was isolated by filtration and rotary evaporation in quantitative yield. Next, 3 g dihydroresveratrol was dissolved in 60 mL of acetone. Four equivalents of cyanogen bromide were added and the reaction was cooled in a dry ice/acetone bath to about -20°C. 3.3 equivalents of triethylamine were added and the reaction was kept between -10°C and -20°C for the duration. Immediately upon addition of TEA, a white precipitate began to form. The reaction was allowed to proceed for 1.5 hours, at which point TLC showed the reaction to be incomplete. At this point an additional 0.5 equivalents of each reagent were added, and the reaction was complete after an additional 30 min. The reaction mixture was then poured into 120mL water to precipitate the product as a white solid. The solid was extracted with two aliquots of 100 and 50 mL of water, respectively, the extracts combined and then washed with two 100mL portions of water and one 100 mL portion of brine. The organic layer was dried over MgSO4, filtered and concentrated on a rotovap until incipient crystallization. The solution was then placed in a -30 °C freezer overnight to yield 2.12 g of white crystals. Concentration of the supernatant followed by cooling yielded an additional 1.08 g of product for a total of 3.20 g (80%). The synthesis was effectively scaled up to the 12 g scale using this method.

4.2 Characterization and Analysis

4.2.1 Test Sample Preparations. Monomeric samples were degassed along with a silicone mold at 20 °C above the melting point and 300 torr prior to use, except when sample melting points were higher than 130 °C, in which case only the silicone mold was degassed at 95 °C and 30 torr. Sample discs measuring 12 mm in diameter x 1-3 mm thick were fabricated by pouring the uncatalyzed monomer into the mold and curing under flowing nitrogen for 1 hr at 150 °C (when permitted by a sufficiently low melting point) followed by 24 hours at 210 °C. The temperature ramp rate during cure was 5 °C / min. The resultant discs weighed 0.2-0.4 mg.

4.2.2 Physical Analysis. Differential scanning calorimetry was performed on ~10 mg samples of monomer reserved after de-gassing using a TA Instruments Q200 calorimeter under 50 mL / min. of flowing nitrogen. Samples were heated to 350 °C, cooled to 100 °C and re-

heated to 350 °C, all at 10 °C / min. The discs were tested via dynamic thermomechanical analysis (dynamic TMA) with a TA Instruments Q400 series analyzer under 50 mL/min of nitrogen flow. The discs were held in place via a 0.2 N mean compressive force with the standard ~5 mm diameter flat cylindrical probe while the probe force was modulated at 0.05 Hz over an amplitude of 0.1 N and the temperature was ramped to 350 °C at 10 °C / min. These rapid heating rates were needed to minimize post-cure of the samples during testing. The thermal lag for each sample was determined (using temperature limits of 100 °C and 200 °C) and used to correct the TMA thermocouple readings (typically by about 5 °C) via a temperature cycling procedure described in detail elsewhere.[14] Infrared analysis was performed by Attenuated Total Reflection Fourier Transform Infrared (ATR-FTIR) spectroscopy using a single bounce diamond ATR crystal. The instrument used was a Nexus 870 FTIR spectrometer with a liquid N_2 cooled mercury cadmium telluride (MCTA) detector. Each spectrum is an average of 28 scans at 4 cm^{-1} resolution.

4.2.3 Analysis by TGA-FTIR. Thermal gravimetric analysis (TGA) - Fourier transform infrared (FTIR) analyses were performed using a Nicolet Nexus 870 FTIR spectrometer interfaced by a heated gas cell and transfer line (held at 150 °C) to a TA instruments Q50 TGA. The FTIR was programmed to acquire a spectrum every 10 seconds integrating 8 scans per spectrum, 256 scans for the background. The detector type was a liquid nitrogen cooled MCTA and the resolution was set at $4cm^{-1}$. The TGA was set to ramp the temperature at 10° C/min to 200°C then 2 °C/min to 400 °C.

4.2.4 Differential Scanning Calorimetry (DSC) at AFRL. ~5 mg samples in powder or solid flake form were placed in a TA Instruments Q200 differential scanning calorimeter under 50 mL/min of flowing N_2. Samples were heated and/or cooled at 10 °C/min, to a maximum temperature of 350 °C. Sapphire discs were used to calibrate the heat flow measurements, and indium was used to calibrate the temperature. Baselines were determined by linear connection of the curves before and after event (such as cure) responsible for individual peaks in the thermograms.

4.2.5 Oscillatory Thermomechanical Analysis (OTMA) at AFRL. Cured discs 11 – 13 mm in diameter x 1 – 3 mm thick and weighing 200 to 400 mg were analyzed in a TA Instruments Q400 thermomechanical analyzer in dynamic mode under 50 mL/min of nitrogen flow. The discs were held in place via a 0.2 N initial compressive force with the standard ~5 mm diameter flat cylindrical probe while the probe force was modulated at 0.05 Hz over an amplitude of 0.1 N (with a mean compressive force of 0.1 N) and the temperature was ramped twice (heating and cooling) between 100 °C and 200 °C (to determine thermal lag) with a final heating to between 200 - 400 °C, all at 10 °C/min. The details on the method of correcting for thermal lag have been published previously.[14]

4.2.6 Density Measurements. Cured discs 11 – 13 mm in diameter x 1 – 3 mm thick and weighing 200 to 400 mg were placed in solutions of deionized water at 19 °C containing $CaCl_2$. The $CaCl_2$ content was adjusted (by means of adding pre-calibrated reference solutions and mixing until homogenized) until a change in buoyancy (floating to sinking or vice versa) was achieved. After a single in change in buoyancy was observed, a sufficient amount of the appropriate reference solution was added to revert to the original buoyancy, then the $CaCl_2$ content was again adjusted by minute increments until neutral buoyancy was achieved. (This

procedure allows for multiple estimates of the $CaCl_2$ content needed to achieve neutral buoyancy, thereby providing a means of checking for consistency.) The neutrally buoyant solution was then transferred into a 10.00 mL volumetric flask, and 10.00 mL of the solution was weighed to 0.0001g. As a further check, the $CaCl_2$ content for the neutrally buoyant solution was calculated and a theoretical density was obtained based on values reported in the literature.[15] A measurement was considered valid only if all experimental and theoretical estimates of density agreed to within 0.003 g/cc. The standard error of measurements using this technique was around 0.001 g/cc.

4.2.7 Hot Water Exposure Testing. discs 11–13 mm in diameter x 1 – 3 mm thick and weighing 200 to 400 mg were placed in solutions of deionized water at 85 °C for 96 hours. The samples were weighed before and after exposure, and in some cases, the sample dimensions were measured to 0.1 mm via micrometer, to ensure that erosion of these samples did not take place during exposure.

4.3 Composite Fabrication

4.3.1 Materials. The bio-based cyanate ester was a mixture of 15% methyl and 85% propyl esters of cyanated resorcylic acid synthesized at NAWCWD China Lake and supplied as a precipitated powder. The reinforcement used was Hexcel S2-glass fabric (style #4522, supplied as a 30" roll with F81 finish). Style #4522 is a plain weave made two twisted 204-filament strands of 9 μm diameter ("G" fiber), with a nominal ply thickness of 0.13 mm and a nominal weight of 123 g/m^2. For fabrication, pristine glass cloth was cut into 102 mm x 102 mm plies in the proper set of orientations needed for fabrication.

4.3.2 Laminate Fabrication. Batches of resin were melted at approximately 80 °C in a vacuum oven under ambient pressure. The molten resin was then de-gassed for a few minutes under approximately 700 mm Hg vacuum. Using a metal frame over a Kapton polyimide liner sheet to prevent slippage, individual plies were oriented and placed in the frame, then approximately 0.5 g of resin was poured into the center of each frame. Using a hot rubber compaction blade, the resin was carefully spread out and worked into the glass ply by hand. The resin was observed to wet the glass readily. After all plies were added, a final liner sheet of Kapton was carefully placed over the assembly, and pressed gently into the laminate using the rubber compactor (working outwards from the center) to eliminate gaps and wrinkles. The entire assembly was then placed in a press pre-heated to 95 °C. No solidification of the resin was observed during the process. The press was then heated to 150 °C and held at ambient pressure for 1 hour to allow for complete flow and wetting, then heated to 225 °C and held for 3 hours under pressure to accomplish gelation and cure. Following cure, the press was slowly cooled to room temperature and the solidified part dislodged. Two types of laminates were fabricated, an 8-ply all 0° laminate held under 15 psi of pressure, and a 16-ply balanced 0°/-45°/+45°/90° laminate held under 30 psi during cure. The target fiber content was about 55% by weight.

5. Results and Discussion

5.1 Cyanate Esters from Creosote Bush Extracts

The initial focus of this project was the conversion of mixed phenols derived from the leaves and stems of the creosote bush (*Larrea Tridentata*) to cyanate ester prepolymer solutions that could then be converted into thermosets with suitable high temperature performance. The crude organic material which was collected in the local area of Ridgecrest, California, was extracted with a variety of solvents including chloroform, ethanol, methanol, and acetone. The chloroform extract was treated with cyanogen bromide and triethylamine to yield an oil. FT/IR analysis of this oil showed characteristic peaks for cyanate ester and cyanurate, as shown below in Figure 4. The upper spectrum is of the creosote extract, and shows peaks for phenolic groups at 3200-3500 cm^{-1} but no outstanding peaks in the 2200-2400 cm-1 region characteristic of cyanate ester monomers or at 1370 cm^{-1} and 1565 cm^{-1} characteristic of polycyanurates. In the lower spectrum, which was measured after treatment with cyanogen bromide, both the cyanate ester monomer and polycyanurate characteristic peaks are present to a large extent, indicating that a partially polymerized cyanate ester (a "prepolymer" has formed.) Unfortunately, the oil that is isolated from this reaction has a short and variable pot life depending on the particular extract used. The propensity of this material to spontaneously polymerize greatly reduces its utility as a resin system.

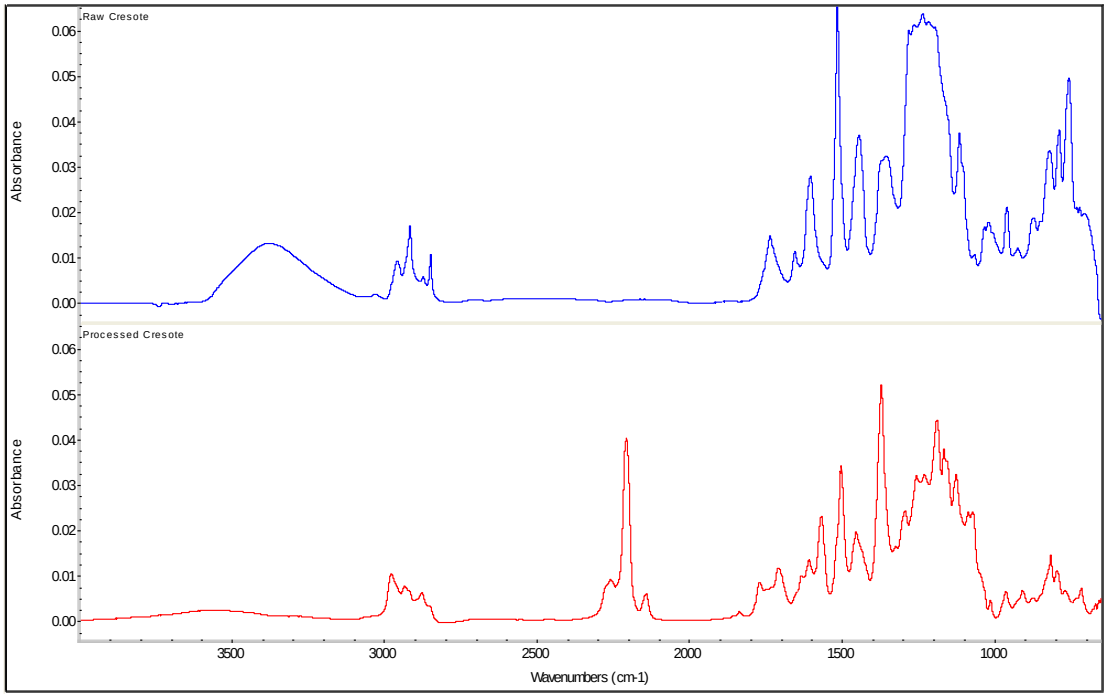

Figure 4. FTIR of the chloroform extract of creosote leaves and stems (top) and residual oil after treatment with cyanogen bromide and triethylamine (bottom).

To evaluate pure NDGA as a resin precursor, substantial effort was expended to isolate NDGA from the crude extract with an eye toward further synthetic work that would allow for a well-defined cyanate ester monomer. We did not evaluate the utility of column chromatography for this system given the large amounts of waste solvent produced in this process. Simple fractional crystallization did not result in pure NDGA, but a fractional extraction method with a basic aqueous solution was capable of yielding the pure phenol in moderate yield. Treatment of NDGA with cyanogen bromide and triethylamine resulted in a colorless residue that was insoluble in all common organic solvents. Although solution phase NMR spectroscopy could not be performed, FT-IR (shown in Figure 5) showed the characteristic resonances for cyanurate ring and also residual cyanate ester. The upper spectrum in Figure 5 is that of pure NDGA; the lower

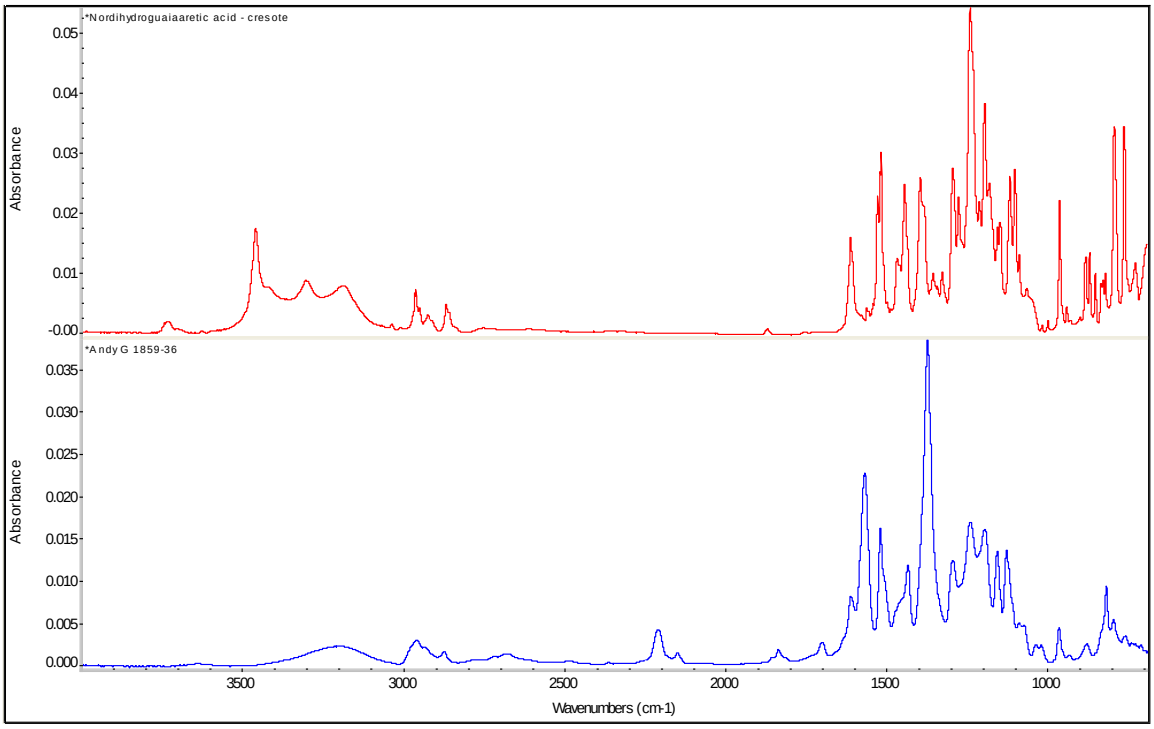

Figure 5. FTIR spectrum of NDGA (top) and NDGA treated with cyanogen bromide and triethylamine (bottom).

spectrum is from the solid formed after treating NDGA with cyanogen bromide. The most prominent peaks appear at 1370 cm^{-1} and 1565 cm^{-1} and are characteristic of polycyanurates. A small set of new peaks is also visible at 2200-2400 cm^{-1}, indicating some residual cyanate ester groups remain in the solid. It is proposed that NDGA, which has ortho phenolic groups, forms an imidocarbonate intermediate which then reacts with a nearby imidocarbonate to form a triazine ring. This reaction precludes the isolation of a discrete cyanate ester and renders both purification and fabrication steps difficult. In light of the perceived difficulties in utilizing NDGA rich phenolic mixtures as feedstocks for cyanate esters, we explored the use of other polyphenolic structures focusing initially on bis-phenols derived from lignin.

5.2 Vanillin as a Feedstock for High Performance Cyanate Esters.

High performance polymeric composite resins, whether a polyimide, cyanate ester, *bis*malimide, or similar, are based upon a network of aromatic structures.[16] Hence, to create a series of new high performance polymeric resins based on a renewable bio-aromatic feedstock we have selected vanillin as our starting point. In this paper, we explore different methods of making vanillin based "dimers" followed by conversion of these compounds to make a series of *bis*(cyanate) esters. Details are presented for the synthesis and curing chemistry of three new vanillin-based *bis*(cyanate) esters as well as a look at physical properties of the cured resins.

5.3 Synthesis of bis-Phenols and Corresponding Cyanate Esters.

As a first attempt at making bis-cyanate esters from vanillin, we explored an oxidative coupling route. Reduction of the carboxaldehyde group in vanillin to yield 4-methyl-2-methoxyphenol in nearly quantitative yield has been demonstrated in the literature.[17] Based on the lack of extraneous reactive functional groups, this molecule was chosen as a starting point. Although the literature abounds with reports on methods for coupling the phenolic rings of 4-methyl-2-methoxyphenol,[18] a procedure detailed by Marques and coworkers[19] uses the methylene chloride soluble permanganate reagent, $MeBu_3NMnO_4$, to provide a clean conversion to the vanillin-biphenyl product (**1**) (Scheme 3). Although the crude yield of **1** is excellent, losses during purification resulted in comparable yields (~50%) to those reported in the literature. Suitably pure **1** was readily converted to the *bis*(cyanate) ester **2** in high yield (~85%) by treatment with cyanogen bromide in the presence of base.

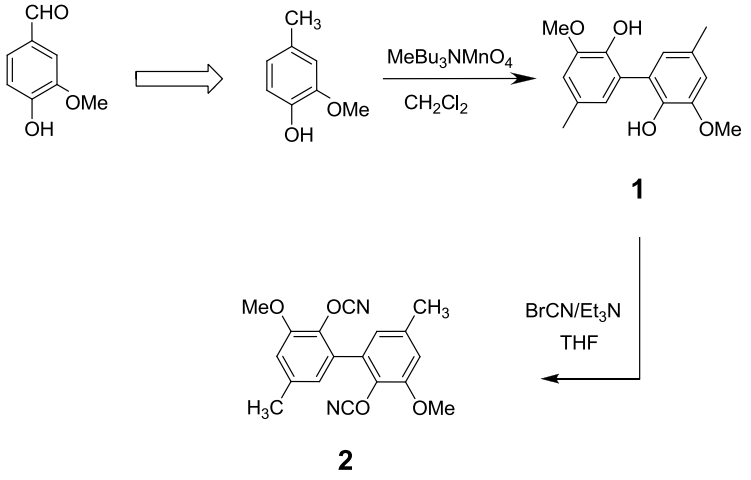

Scheme 3. Conversion of vanillin to (2)

Since there is little data in the literature concerning 2,2'-bis(cyanato)-1,1'-biphenyl derivatives, we invested the time to prepare model compounds **3** and **4** (Scheme 4). Recently a chiral version of compound **4** was prepared although no cure chemistry of the cyanate ester was

reported.[13] As a result, the ability of monomer **4** to form a complete triazine network (i.e. fully cured resin) was not established.

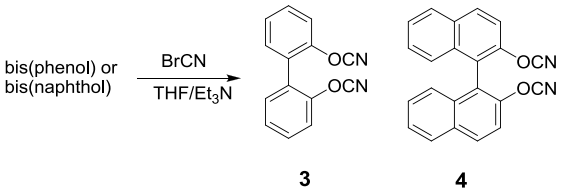

Scheme 4. Synthesis of (3) and (4)

As an alternate approach, we attempted to couple vanillin by means of a reductive coupling of the aldehyde group. Although vanillin has been reported as a substrate that is recalcitrant to reductive coupling by low valent metal species, the bis(phenolic)ethene (**5**) was isolated in good yield through a McMurry coupling without protection of the phenols (Scheme 3).[20] Compound **5** was then hydrogenated over palladium on carbon to form the saturated bis(phenolic)ethane (**6**) in high yield (~90%). Conversion of **5** and **6** to their respective cyanate esters **7** and **8** was then carried out by treatment with cyanogen bromide in the presence of base (Scheme 5).

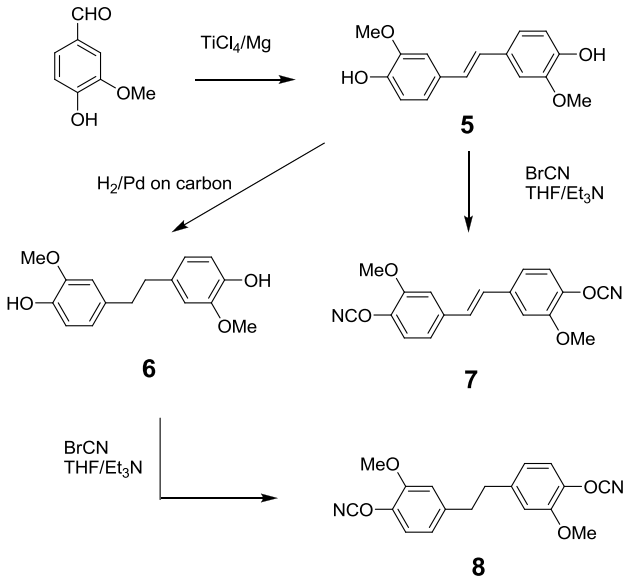

Scheme 5. Reductive coupling of vanillin to produce bis-phenols and ultimately cyanate esters (7) and (8).

5.4 Solid State Structures of Selected *bis*(cyanate) Esters.

Information gleaned from single-crystal molecular-structures can aid the chemist in revealing the most important intra- and inter-molecular interactions in the solid state for a given series of organic molecules. The strength of intermolecular interactions ultimately defines the

melting point of a solid and to a lesser extent, defines the predominant intermolecular interactions and/or collision orientations in the melt. To better understand the factors leading to successful and complete thermal cure of cyanate esters in the melt, we investigated the solid state structures of selected cyanate esters.[21]

Table 1. Selected crystallographic data and structure refinement parameters for **4**, **7**, and **8**.

Identification code	**Compound**		
	4	**7**	**8**
Empirical formula	C22 H12 N2 O2	C18H14N2O4	C18H16N2O4
Formula weight	336.34	322.31	324.33
Crystal system	monoclinic	monoclinic	monoclinic
Space group	P2(1)	P 1 21/c 1	P 1 21/c 1
Unit cell dimensions	a = 7.5666(7) Å α= 90° b = 15.6091(15) Å β= 99.466(2)° c = 7.4520(6) Å γ = 90°	a = 3.8785(4) Å α = 90° b = 12.2362(13) Å β = 95.908(2)° c = 16.2071(17) Å γ = 90°	a = 4.3999(2) Å α = 90° b = 12.3001(9) Å β = 97.5910(10)° c = 14.8279(11) Å γ = 90°
Volume	1642.4(3) $Å^3$	765.07(14) $Å^3$	795.44(10) $Å^3$
Z	4	2	2
Density (calculated)	1.360 g/cm^3	1.399 g/cm^3	1.354 g/cm^3
Crystal size	0.40 x 0.35 x 0.10 mm^3	0.11 x 0.12 x 0.27 mm	0.07 x 0.20 x 0.28 mm
Theta (max)	25.08°	25.49°	25.50°
Reflections collected	17,921	8435	8832
Reflections 'observed'	3498 [I>2σ(I)]	982 [I>2σ(I)]	1124 [I>2σ(I)]
Independent reflections	5801 [R(int) = 0.0456]	1432 [R(int) = 0.0311	1481[R(int) = 0.0265]
Data / restraints / parameters	5801 / 0 / 469	1432/0/110`	1481/0/110
Goodness-of-fit on F^2	0.863	1.048	1.025
Final R indices [I>2σ(I)]	R1 = 0.0448, wR2 = 0.1437	R1 = 0.0416 wR2 = 0.0961	R1 = 0.0354 wR2 = 0.0842

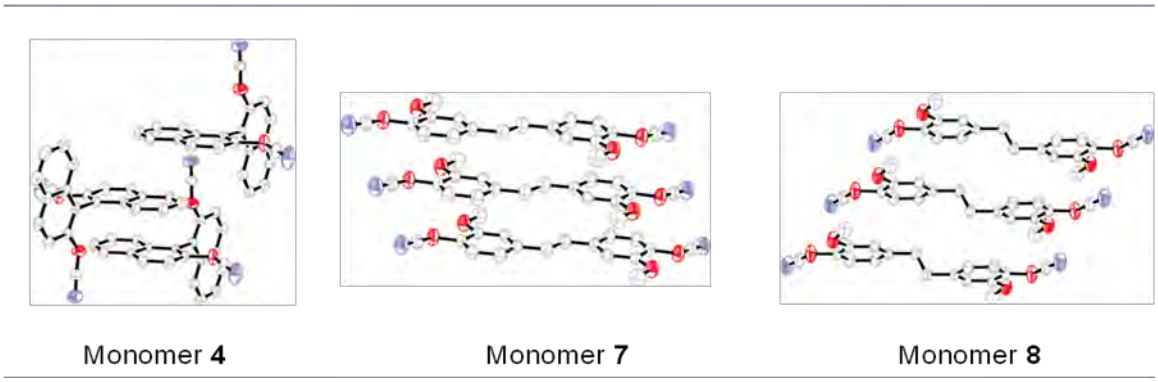

Figure 6. ORTEP drawings of 2,2'-*bis*(2-cyanato)-1,1'-naphthyl) (**4**), 1,2-*E*-*bis*(4-cyanato-3-methoxyphenyl)ethene (**7**), and, 1,2-*bis*(4-cyanato-3-methoxyphenyl)ethane (**8**) taken from the single-crystal x-ray diffraction molecular-structure determinations.

Suitable single-crystals for x-ray diffraction studies could be obtained for **4**, **7**, and **8**. Table 1 presents selected crystallographic data for the molecular structure determinations and in Figure 6 we present ORTEP drawings that illustrate the packing arrangement for each of the monomers.

Although in general, the bond lengths and angles in the solid state structures of **4**, **7**, and **8** are quite typical of cyanate esters, we sought to determine the extent to which intermolecular

forces in these molecules impacted the melting points and ultimately the cure chemistry of these resins. Given that efficient curing can only occur in the liquid phase, a lower melting point is beneficial as it translates into a larger processing window for the material. Although **7**, **4**, and **8** have similar molecular weights and polarities, their melting points of 237, 205, and 190 °C, respectively, are quite disparate. Starting first with **7**, a completely planar molecule, one can observe that the aromatic rings stack on top of each other with a centroid-to-centroid distance of 3.879(3) Å and an interplanar distance of 3.552(3) Å. The considerable degrees of freedom associated with the saturated methylenes linking the aromatic rings in monomer **8** leads to a much longer centroid-to-centroid distance of 4.400(2) Å; however, a similar interplanar distance of 3.520(2) Å. Compound **4** is unique among these molecules as it has orthogonal aromatic systems. Although two independent molecules are present in the unit cell and multiple stacking interactions are present, the shortest centroid-to-centroid distance is 3.619(6) Å with a corresponding interplane separation of only 3.43(2) Å. The cyanate esters also appear to interact with the aromatic rings with non-bonded contacts as low as 3.142(6) Å between nitrogen and select aromatic carbons. These close non-bonded contacts are offset by the relatively inefficient packing of non-stacked aromatic systems. The strength of the intermolecular forces in these systems may also be qualitatively supported by the densities of the solids. Compounds **7**, **4**, and **8** have densities of 1.399, 1.360, and 1.354 g/cm^3, respectively, and this trend directly corresponds to the decrease in observed melting point (vide supra).

5.5 *bis*(vanillin cyanate ester) Curing Chemistry.

We first explored the cure chemistry of **2**. DSC analysis of **2** shows a somewhat broad melting point at 205°C, followed by an exotherm of 400 J/g (or 65 kJ/mol-equiv of cyanate ester) and a peak cure temperature near 270°C. The in-situ cure appears to start immediately upon melting, in line with the observations from sample molding. The exotherm also appears insufficient for full cure of the cyanate ester groups[22] which should produce 100 kJ/mol-equiv of cyanate ester. Furthermore, the T_g after in-situ cure of around 175 °C is 50-100°C lower than what is expected based on full cure of *bis*(cyanate) esters with a similar cross-link density and architecture. After 24 h at 210°C, the as-molded sample showed a residual cure of around 12 kJ/mol-equiv cyanate ester with a T_g near 195°C. The latter result indicates a more extensive however still incomplete cure.

Numerous attempts were made to degas and cure the vanillin monomer **2** using both slow and rapid heating under both partial vacuum, and high vacuum with temperatures ranging from 100 – 200 °C. In all cases some nitrogen atmosphere was applied to the samples under heating. For all attempts, the bis(cyanate ester) **2** is found to cure essentially concurrent with melting and this leads to samples which show incomplete consolidation. During the curing and heating process it appears there is a release of volatiles which is evidenced by bubbles within the cured samples. Thus for **2,** we find that fabrication of void-free samples is quite difficult if not impossible.

In order to improve processing characteristics of *bis*(cyanate) ester monomer **2**, we blended it at ~35 wt-% into Primaset® LECy. The latter is the bis(cyanate ester) prepared from Bisphenol E and exists as a super-cooled liquid at room temperature. After some stirring the bis(cyanate ester) monomer **2** is readily dissolved and forms a homogeneous mixture. The mixture is then degassed at 95 °C and cast into a silicone mold. This is followed by heating at 150 °C for 1 h and 210 °C for 24 h under flowing nitrogen to affect cure. A strong solid sample was formed, and although thin samples were homogeneous, bubbles could be seen in samples

thicker than ~ 1 mm. Hence, even as a blend, significant volatiles were generated during the cure reaction and then became trapped within the fully cured sample.

Examining the cure chemistry of monomer **2** by thermal gravimetric analysis (TGA) supports the notion that in addition to cure chemistry above 200 °C there is weight loss of ~15 wt-%. Further heating shows a leveling off of weight loss and not until over 300 °C do we observe a second and more dramatic weight loss from the cured resin. After the exotherm and weight loss stops again we have a char-yield of ~50 wt-%. The char yield corresponds to essentially turning monomer **2** into a graphite-like material with all the side groups removed from the biphenyl rings during the final exothermic event.

To further elucidate the reasons behind this early weight loss we utilized TGA/ FTIR spectroscopy to analyze the thermal cure of monomer **2** (Figure 7). What is very apparent in the heating/curing of monomer **2** is that at the melting point/cure point (~200 ^{o}C) we see evolution of isocyanic acid (Scheme 6). This accounts for the initial weight loss and explains the difficulty in obtaining void free resin bars. Monomer **2** is purified and recrystallized in a manner to avoid and eliminate water contamination; however, we cannot rule out unambiguously that some water may indeed be trapped within the crystalline lattice.

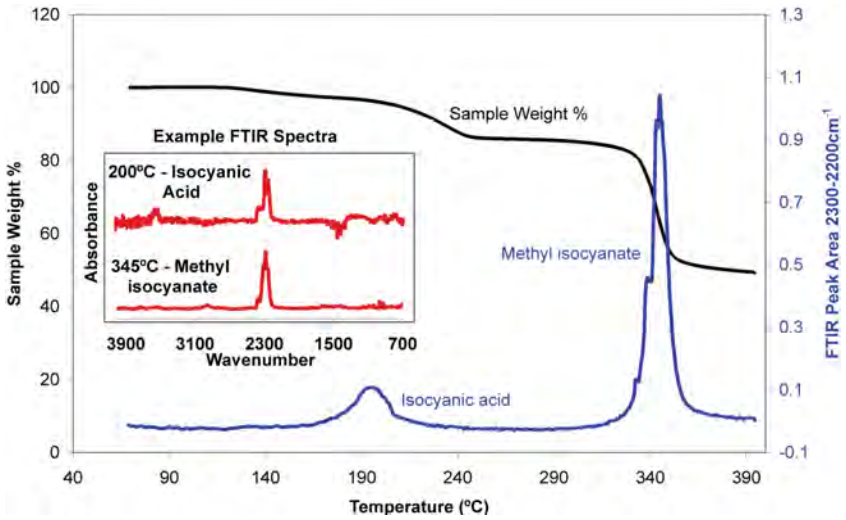

Figure 7. TGA/FTIR analysis for compound 2.

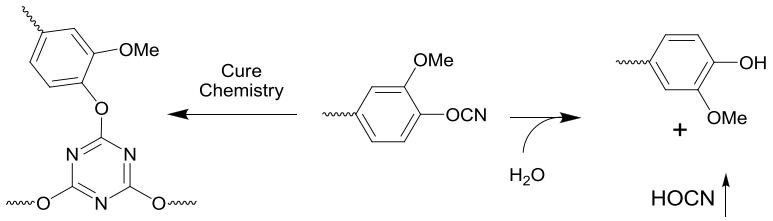

Scheme 6. Proposed mechanism for the decomposition of methoxy functionalized cyanate esters

The second weight loss occurring above 300 ^{o}C is a bit more interesting. It appears that the ortho-methoxy group is combining with the cyanate ester group to form methyl isocyanate (MeOCN) (Scheme 7). This most likely occurs through some kind of intramolecular transfer of the methyl group to the cyanate ester oxygen. It could occur as the triazine ring thermally-depolymerizes and thus effectively drives the equilibrium by evolution of methyl isocyanate. Alternatively, the methyl transfer could occur in the triazine structure to afford the methoxy-substituted derivative that then reacts to release the methyl isocyanate (bottom sequence in Scheme 7).

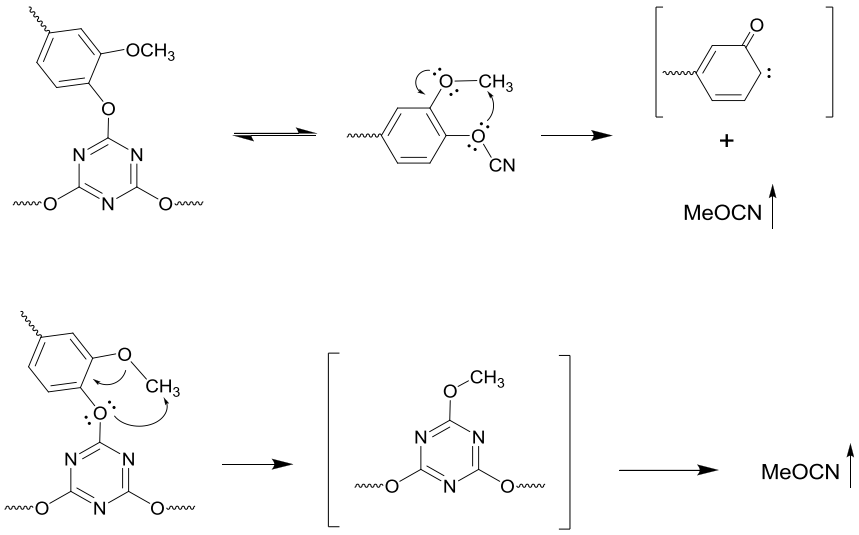

Scheme 7. Decomposition mechanisms for cured cyanate esters at elevated temperature

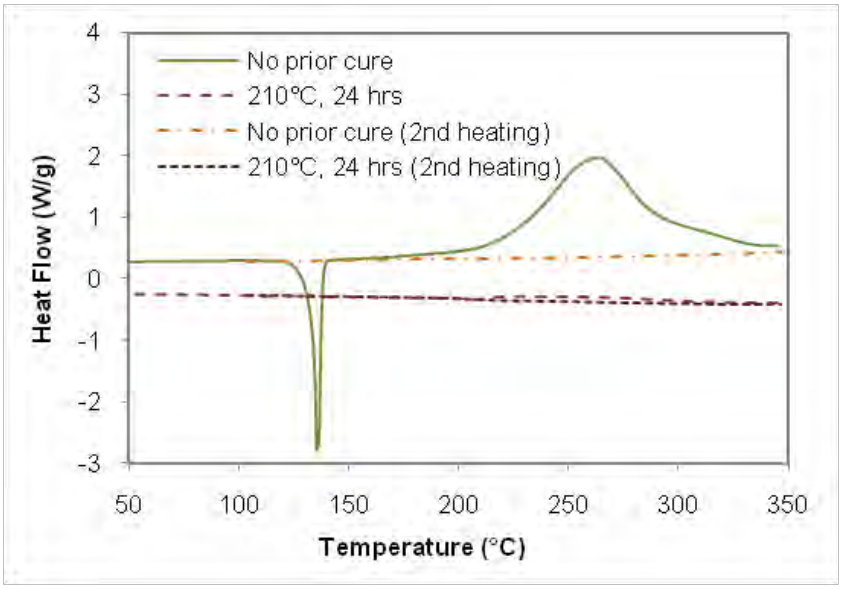

Figure 8. DSC data for various initial and post curing cycles of monomer **3** .

DSC analysis for the thermal cure of the biphenyl monomer **3** is shown in Figure 8, for the resin before and after *in-situ* cure, as well as before and after residual cure for samples molded at 210 °C for 24 h. The biphenyl cyanate ester has a distinct melting point at 135 °C, then exhibits a typical exotherm for cyanate esters with a peak temperature around 260 °C and an enthalpy of cyclotrimerization near the expected value of 100 kJ/mol-equiv cyanate ester. In contrast, we find that after 24 h at 210°C the molded sample shows only a residual cure of ~6 kJ/mol-equiv cyanate ester. Since there is no guarantee that 100% conversion is achieved even after residual cure, the DSC data is consistent with a conversion of less than ~94% for the as-molded sample. The observed glass transition temperatures are around 210°C for all cured samples. FT-IR analysis of the as-molded biphenyl cyanate ester clearly shows disappearance of the monomer and appearance of strong cyanurate peaks with conversion estimated at 80-95%.

An analogous DSC analysis of the binaphthyl monomer **4** indicates a reduced enthalpy of cure of 70 kJ/mol-equiv cyanate ester, a peak cure temperature of only 210°C, and a somewhat larger residual cure after exposure to 210°C for 24 h (5 kJ/mol-equiv cyanate ester). For this monomer we observe a glass transition temperature of around 210°C for *in-situ* and as-molded cure and 230°C after residual cure. Analysis of FT-IR spectroscopic data of the as-molded binaphthyl cyanate ester resin indicate a lower degree of conversion (45-75%) compared to the biphenyl monomer **3**.

Taken together, the DSC and FT-IR data suggest that less than complete cure is achieved for as-molded biphenyl and binapthyl bis(cyanate) ester resins. Based on previously reported data for bis(cyanate) esters, including those containing naphthyl groups,[23] an estimate for the expected glass transition temperatures would be 0°C for the uncured monomer and 300°C for a fully cured resin. By applying the diBenedetto equation as a method to accurately predict T_g values for intermediate conversions it can be concluded that our observed T_g values of 210-230°C correspond to conversions of 80-85%.[24] Thus it seems more likely, for both the biphenyl and binaphthyl monomer systems, that the FT-IR estimates for conversion are approximately correct and that full cure cannot be achieved even when samples are subsequently heated to 350°C in the DSC. Although the biphenyl bis(cyanate) ester exhibited an exotherm sufficient to account for complete *in-situ* cure of a DSC sample, the post-*in-situ*-cure T_g is not consistent with complete network formation; in which side reactions or formation of non-network structures may be present. The brittleness of the as-molded specimens is another indication that network formation is not complete for these biphenyl and binaphthyl systems.

The difficulty in forming thermoset network polymers with an expected glass transition temperature greater than ~300 °C for the biphenyl and binaphthyl CEs may result from steric hindrance around the cyanate ester groups, as well as from the contorted nature of the tricyanate networks formed. In particular, once the T_g of the cured network becomes higher than the cure temperature, any additional cyclotrimerization will require a favorable arrangement of multiple cyanate ester groups. Such arrangements seem especially unlikely for the cyanate esters under consideration. Such an effect would explain the prevalence of a T_g of 210 °C in the as-molded samples.

The thermal curing of monomer **7** became an interesting exercise. DSC analysis of the monomer powder shows a sharp melting transition at 237 °C a large enthalpy of melting of 230 J/g along with a melt-triggered exotherm of 160 kJ/mol-equiv cyanate ester. Since this value is considerably larger than typically seen for curing of the cyanate ester groups, it is likely that additional chemical reactions take place concomitant with cyclotrimerization. After heating the sample and allowing the cure/reaction chemistry to finish we observe no glass transition in the

DSC curve. As expected, when a sample of **7** was loaded in to a silicone mold large enough to accommodate compaction and was then heated to 150 °C at 300 torr under a nitrogen purge, no consolidation of the sample was observed. Further heating of the sample to 210 °C under 15 psi of nitrogen also resulted in no visible consolidation of the sample. After 24 h at 210 °C, the partly consolidated sample was removed from the mold and analyzed by FT-IR spectroscopy. The FT-IR data indicate a conversion of 50-70% based on the disappearance of the cyanate ester monomer band; however, the cyanurate peaks in the spectrum were somewhat smaller than expected.

In contrast, samples of monomer **8** are found to consolidate and cure in a much more favorable manner. The DSC of monomer **8** was more typical of easily processed cyanate esters, although the observed melting point of **8** near 190 °C is higher than normal and results in a smaller, though still ample, process window, with a cure exotherm commencing shortly after the sample appears fully melted. The DSC measured cure exotherm of 92 kJ/mol-equiv cyanate ester is significantly greater than what we have observed for the biphenyl/binaphthyl cyanate esters prepared above. When placed in a silicone mold and heated to 210 °C for 24 h, the sample was able to melt and compact over a period of a few minutes, well before the onset of significant cyclotrimerization, resulting in the formation of a void-free sample as cure proceeded. A DSC analysis of the as-molded sample reveals no detectable residual cure. Moreover, FT-IR analysis indicated an extent of cure of approximately 98%. The high quality of the sample allowed for a more in-depth analysis of the thermomechanical properties of cured **8** via TMA, as shown in Figure 9. The sample shows a peak in the loss modulus at 180 °C and with a corresponding peak in tan-δ of 202 °C.

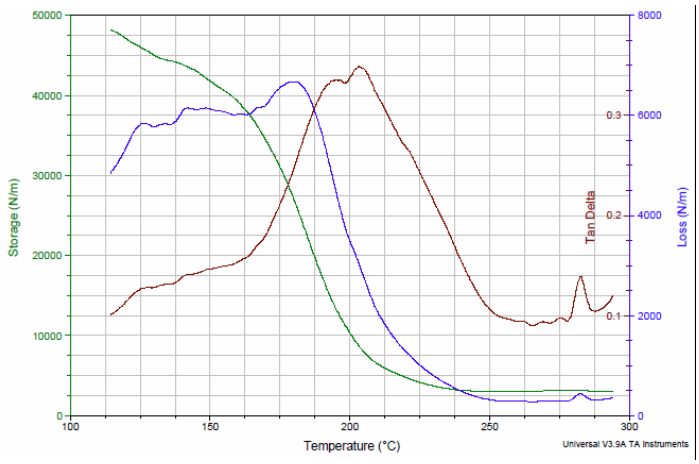

Figure 9. TMA analysis after curing of vanillin bis(cyanate) ester monomer **8**.

We also explored the thermal stability and behavior of monomer **8** using TGA/ FTIR spectroscopy (Figure 10). We find it very interesting that for this cured resin sample, like the biphenyl-vanillin monomer **2,** we observe at high temperature (> 330 ^{o}C) a thermal degradation reaction that leads to formation of methyl isocyanate. Hence, it appears these vanillin based cyanate esters with their ortho-methoxy substituents provide a unique reaction pathway for thermal decomposition. It is important to note that at temperatures below 300 ^{o}C we do not observe this reaction.

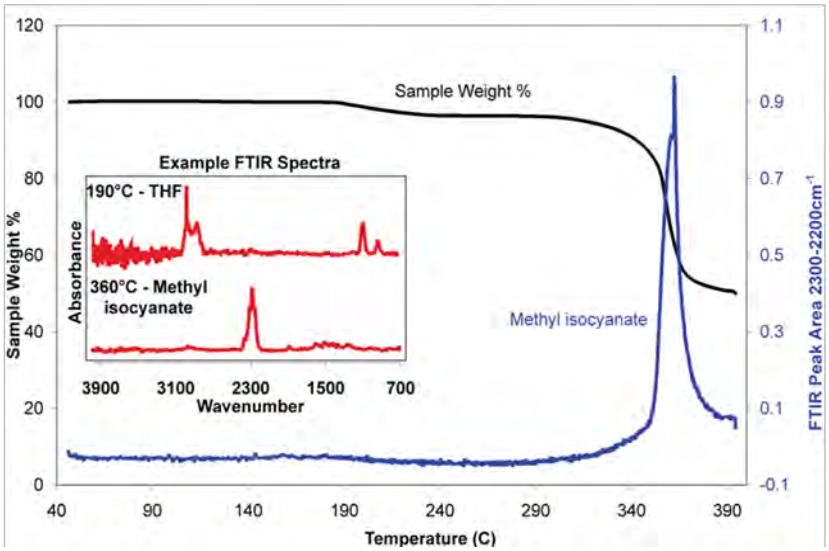

Figure 10. TGA FTIR plot for the thermal heating of monomer **8**. Inset is the FT-IR spectra of the gases produced at the labeled temperature. The initial weight loss is due to residual THF in the sample of **8**.

5.6 Summary of Vanillin Work

In the study we have demonstrated the successful synthesis of three new bis(cyanate) ester monomers based on the biofeedstock of vanillin. We found that direct connection of the vanillin to form a vanillin-biphenyl cyanate ester monomer afforded a material that produced only partial cure and because of a high melting point and the generation of volatiles, provided virtually no processing window. Model studies exploring the cure chemistry of unsubstituted biphenyl and binaphthyl bis(cyanate) esters reveal that in general, this type of chemical architecture does not support a complete cure of the cyanate ester groups. By coupling the vanillin through the aldehyde group, we were able to form two new bis(cyanate) esters that in part allowed us to avoid the cure difficulties associated with the biphenyl-architecture. The unsaturated monomer **7** displayed a very high melting point and as a consequence we observe some cure chemistry concurrent with other unproductive side-reactions. Based on the lack of mechanical properties for the "cured" sample it is apparent that a dense network is not formed. The thermal cure chemistry of monomer **8** is successful and defect free resin-bars can be prepared using standard processing techniques. At elevated temperatures both vanillin resins made from **2** and **8** display an intriguing thermal degradation reaction producing methyl isocyanate. The resin made from **8** by all accounts (spectroscopic and mechanical) appears to have under gone complete cure and displays excellent thermal stability at temperatures below the T_g of 202 ^oC.

5.7 Single Ring bis-Cyanate Esters from Resorcylic Acid

5.7.1 Synthesis of cyanate esters. A common trend in the production of renewable fuels and polymers from biomass is the utilization of bioengineered bacteria to convert low value feedstocks such as hemicellulose or cellulose into high value materials suitable for specialized

applications. Phloroglucinol has been shown to be a viable renewable product that can be produced in this manner. Phloroglucinol can be selectively reduced to resorcinol and then subsequently reacted with K_2CO_3 to produce a mixture of resorcylic acids (Scheme 8). The carboxylic acid group provides a synthetic handle for functionalization (through formation of alkyl esters) which allows for tunable characteristics of the final cyanate ester including such important physical properties as T_g, water uptake, toughness, and flexibility. It should be noted that synthesis of alkyl esters can utilize renewable alcohols such as methanol, ethanol, isopropanol, *n*-propanol, isobutanol, *n*-butanol, *n*-pentanol, etc. The carboxylic acid source can be from waste CO_2, allowing for additional carbon sequestration. In the current work, we used α-resorcylic acid (3,5-dihydroxybenzoic acid) as our starting point. Three cyanate esters were synthesized in excellent yield with R = ethylhexyl, methyl, and propyl, compounds **10**, **11**, and **12** respectively (Scheme 9).

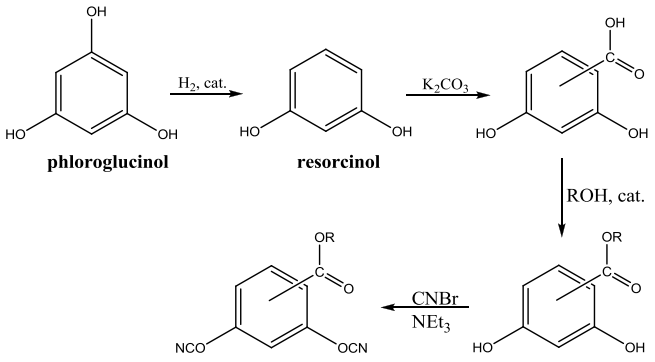

Scheme 8. General synthesis of single-ring bis-cyanate esters from phloroglucinol

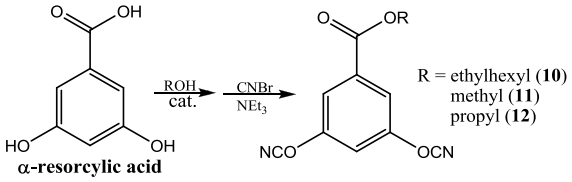

Scheme 9. Synthesis of single-ring bis-cyanate esters studied in this work.

5.7.2 Material testing (Density, Water Uptake)

Density data: The density of **10** was determined to be 1.15 g/cc, while that of **11** was measured at 1.40 g/cc, for cure protocols involving 24 hours at 210°C as the final step. For comparison purposes, most commercial dicyanate esters exhibit a density near 1.2 g/cc. For further comparison, the theoretical densities of the cyanate esters were computed according to the correlation developed by Bicerano.[25] The theoretical densities were 1.10 g/cc for **10** and 1.44 g/cc for **11**, reasonably close to the experimentally obtained values given that a standard deviation of 0.04 g/cc for the difference between predicted and observed densities has been found for the Bicerano correlation.

Water Uptake: For **10**, the water uptake of 0.9% by weight was among the lowest measured for cyanate esters, while for **11**, the water uptake was 8.5% by weight, among the highest measured for cyanate esters. The errors is these measurements are typically 0.1 – 0.2%. A number of factors may be responsible for the vast difference in water uptake, including the hydrophilic character of the methyl ester group versus the hydrophobic character of an ethyl hexyl ether group, a much lower density of cyanurate groups in **10**, and differences in molecular packing. It should be noted that resorcinol dicyanate ester, a compound quite similar to MW-ME, had the highest measured water uptake among cyanate esters known as of the early 1990s.[26]

5.7.3 Thermal Analysis of Single-Ring Cyanate Esters. Figure 11 shows the DSC scan of uncured **10**. The breadth of the cure exotherm and its peak temperature near 200 °C suggest that the system is self-catalyzing, either through the presence of impurities or adventitious water. The meta-substitution pattern on the aromatic ring in the cyanate ester may also activate the system towards cure at a lower temperature, mimicking the effect of catalytic impurities. Also of interest, the enthalpy of cure is measured at just 390 J/g, or a little over 60 kJ/mol, much less than the expected 100 kJ/mol for cyanate ester cure. These data thus suggest that full cure of the system may not be possible due to geometric considerations, a situation seen in other highly asymmetric dicyanate esters with bulky substituent groups.[27] Note also that no melting was evident in the DSC; **10** was a viscous liquid at room temperature.

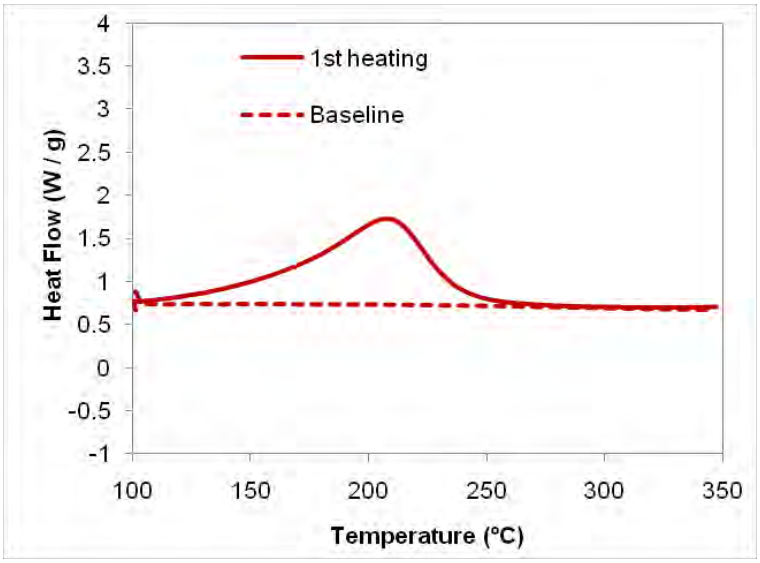

Figure 11. DSC scan of uncured **10**.

For comparison, Figure 12 shows the DSC scan of uncured **11**. The cure exotherm, though still present, shows two quite broad peaks. There is also a second exotherm above 320 °C, though this could be due to degradation or other chemical reactions triggered at high temperature. Ester groups have been shown to catalyze the cure of cyanate esters, thus the very low cure temperature may reflect the chemical composition of the monomer (along with activation effects due to the pattern of aromatic ring substitution) rather than the level of impurities present. Though it is a solid at room temperature, the **11** melts well below 100 °C, leaving an adequate window for processing before the onset of cure. The cure exotherm at low temperature also

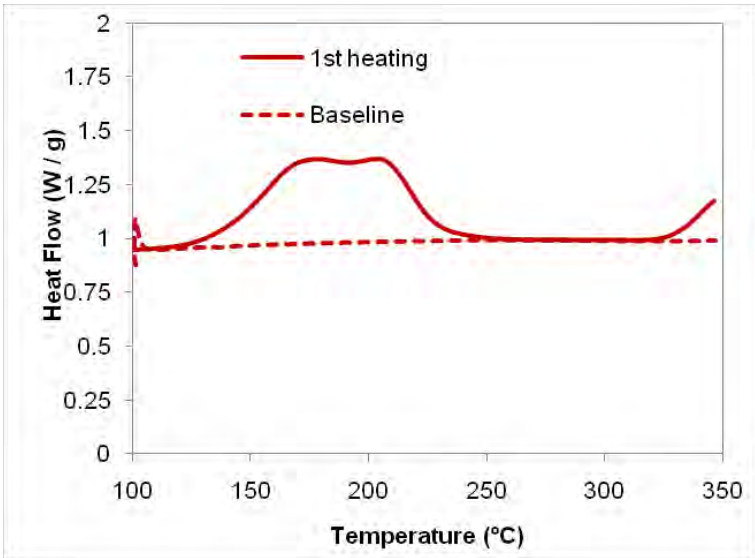

Figure 12. DSC scan of uncured **11**.

seems quite small, however, due to the unusual peak shape present, an alternate means of quantifying the extent of cure was sought.

One alternate means of assessing the degree of cure of a cyanate ester is to measure the extent of residual cure seen in the DSC trace of a cured, rather than an uncured, sample. Figure 13 shows the results of such a DSC experiment for **11**. In this case, the difference between the first heating (after cure of the sample at 150 °C for 1 hr followed by 210 °C for 24 hrs) and the subsequent heating shows a difference of no more than about 10 kJ/mol, corresponding to roughly ~10% residual cure. Although this technique only sets an upper limit for the amount of cure achieved, when combined with TMA data, as described later, it indicates that nearly full (though not complete) cure was achieved. The first heating curve shows some unusual features at about 320 °C, which appear to indicate mechanical instabilities (perhaps due to the generation of volatile species) at around this temperature. Note that the second heating curve is quite featureless, indicating that the residual cure process is captured by the first scan, and that any thermal degradation is limited.

Turning to TMA data, Figure 14 shows the oscillatory TMA scan of **10** cured for 1 hr at 150 °C followed by 24 hrs at 210 °C in nitrogen and subsequently stored under vacuum. Both the final heating and cooling curve are shown in the graph. The T_g values determined from the scan were 152 ± 2 °C for the peak in tan delta, and 135 ± 5 °C for the peak in the loss component of the stiffness. The onset of the change in coefficient of thermal expansion (not shown) took place at 145 ± 1 °C, and the measured coefficient of thermal expansion values were 202 ± 9 ppm / °C at 125 °C (below T_g) compared to a value of 415 ± 0.3 ppm / °C at 175 °C. Note that the uncertainties are based on only two measurements, thus the latter uncertainty is coincidentally low. These T_g values are low for dicyanates with a similar cross-link density (the silicon-containing cyanate ester SiMCy, for instance, has a similar density and molecular volume, yet achieves a T_g on full cure of near 280 °C).[14] Thus, the T_g values may indicate that less than full cure was achieved with the resin, in agreement with the DSC exotherm data. Moreover, the

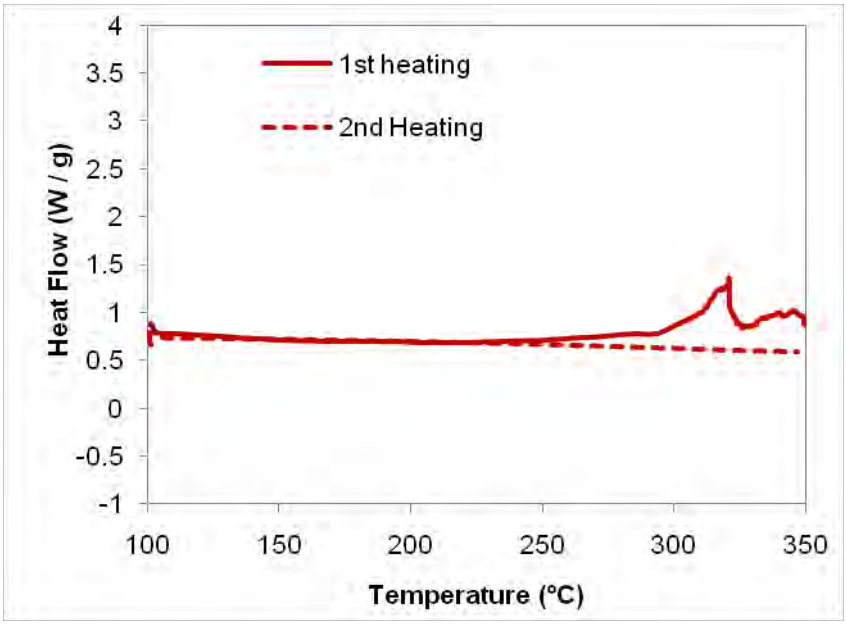

Figure 13. Residual cure of (**11**) as measured by DSC.

coefficient of thermal expansion for fully cured cyanate esters is typically below 100 ppm / °C and typically shows a strong negative correlation with the degree of cure. The observed value of just over 200 ppm / °C below T_g is thus another indication that significantly less than full cure was achieved in **10**. Note than a low extent of cure would also be expected to result in unusually low moisture uptake values, as was observed for **10**.

The response of **10** to exposure to hot water was also quite interesting. As shown in Figure 15, the oscillatory TMA data for samples exposed to 85 °C water for 96 hours indicated

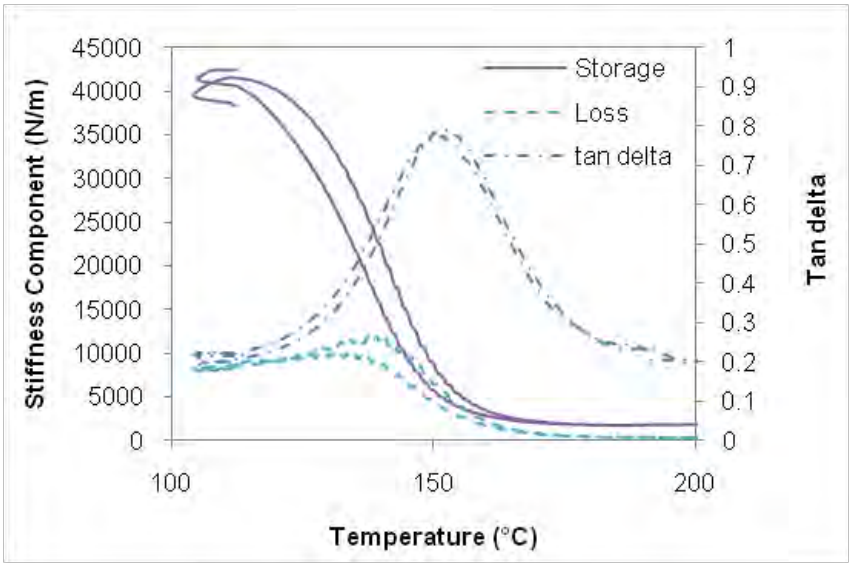

Figure 14. Oscillatory TMA scan of cured (**10**) (dry)

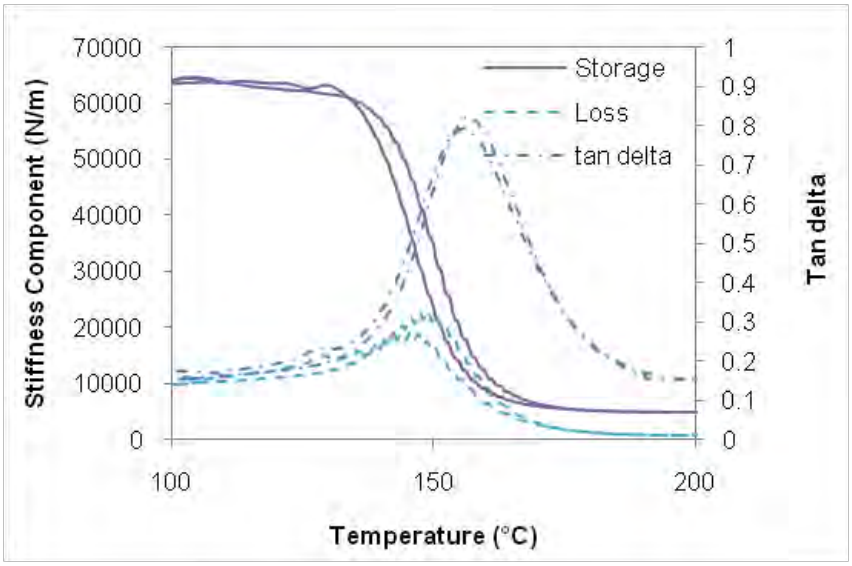

Figure 15. Oscillatory TMA scan of (**10**) after exposure to 85 °C water for 96 hrs.

no decline in T_g, rather, the T_g according to the tan delta peak increased by 4 °C to 156 ± 1°C while the T_g according to the loss peak increased by 12 °C to 147 ± 3 °C. The onset of the change in the coefficient of thermal expansion, however, did decrease to 140 ± 3 °C. Taken together, these data indicate either no change or even a slight increase in T_g took place during exposure to hot water, in stark contrast to most other cyanate esters, which show a decrease, most often of over 100 °C, when exposed to similar conditions. One clue as to why this behavior may take place comes from the coefficient of thermal expansion. It was reduced quite significantly to 130 ± 30 ppm / °C at 125 °C, a decrease of 36%, while increasing by only 5%, to a value of 437 ± 5 ppm/°C, at 175 °C. (The former is below T_g, the latter above it.) These changes are in fact consistent with an increased degree of cure coupled with a modest amount of network degradation.

When an uncured cyanate ester is exposed to water in the absence of catalyst, a temperature of around 200 °C or higher is often needed to induce significant degradation of the uncured groups, however, the water swells the network and the cured groups tend to hydrolyze slowly. Such a process typically results in a net decrease in both the degree of cure and the glass transition temperature of the system. However, in cases where complete cure does not occur due to geometric constraints, the swelling and plasticization created by water ingress may allow for a relaxation of some of the constraints, leading to further cure of the network. This additional cure will raise the glass transition temperature, countering the decrease expected from hydrolysis. The same process should also result in a substantial decrease in coefficient of thermal expansion below T_g, as observed in the system.

The oscillatory TMA data for the dry **11** cured at 150 °C for 1 h followed by 24 hrs at 210 °C is shown in Figure 16. In this case, only the final heating to about 350 °C is shown, since (as is evident by the sudden reversal in the storage signal and the noise in the loss signal), the sample became unstable before the heating could be completed. It should be noted that the onset temperature for this instability was about 315 °C, similar to that seen in the DSC data. Although

no clear peak in either the loss component of the stiffness or tan delta was observed (the pattern suggests that the T_g was at a higher temperature than could be reached), the onset of the change in the apparent coefficient of thermal expansion was measured at 305 °C. Due to the sample instability, however, this value may not reflect the actual glass transition. All that can be said for certain is that the data indicate a T_g of about 310 °C or greater for the fully cured system, in line with expectations for highly cross-linked cyanate esters. The coefficient of thermal expansion below T_g, at 125 °C, was 53 ppm / °C, a number that reflects the expected high density of cross-links in the system. The data in Figure 16 also exhibit subtle step-like features just above 210 °C; these features are typical of systems that undergo residual cure while being heated. Such residual cure could have increased the glass transition temperature of the dry sample by as much as about 50 °C based on the DSC data. Thus, while the fully cured dry T_g of the system was above about 310 °C, the dry T_g, as-cured, may have been as low as about 260 °C. A more detailed examination of multiple samples using a variety of heating rates might be able to elucidate the as-cured dry T_g, provided that mechanical instabilities do not interfere with the measurements.

Figure 17 shows the corresponding oscillatory TMA for **11** after cure (as described earlier) followed by immersion in 85 °C water for 96 hrs. The T_g according to the peak in tan delta fell to 175 ± 1 °C while the T_g according to the loss peak fell to 165 ± 1 °C, and the T_g according to the step change in coefficient of thermal expansion fell to 144 ± 3 °C. Note that the pattern of these differences, with the coefficient of thermal expansion giving a T_g value about 20 °C lower than that found via the oscillatory response, and with the peak in loss a few degrees lower than the peak in tan delta, is very typical of thermosetting resins. The coefficient of thermal expansion at 125 °C increased slightly, to 66 ± 1 ppm / °C, as a result of the break-up of the network associated with hydrolysis. The very large drop in T_g on exposure to water is a likely consequence of the very high cross-link density in the material combined with the large amount of water uptake observed, as well as the self-catalyzing nature of the material. The "wet" T_g values are still, however, considerably better than epoxy resins though somewhat lower than commercially available dicyanate esters.

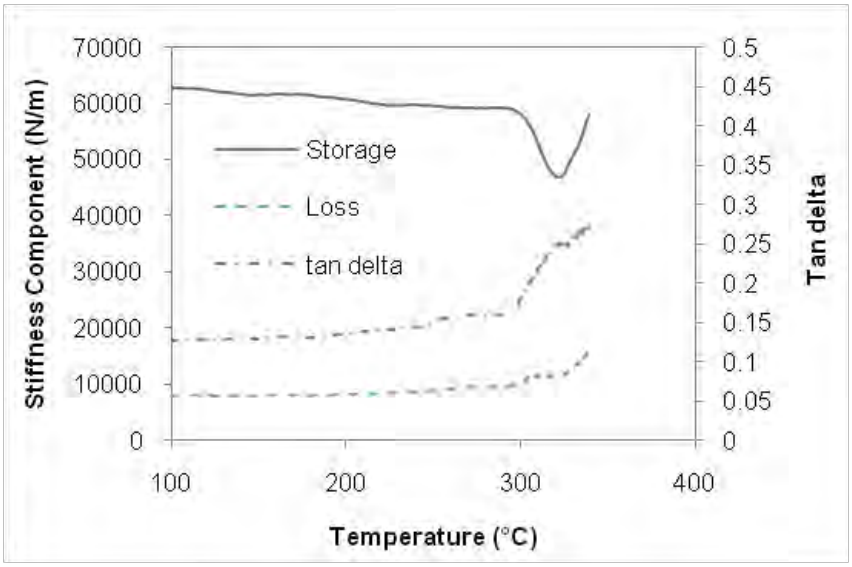

Figure 16. Oscillatory TMA of cured (**11**) (dry).

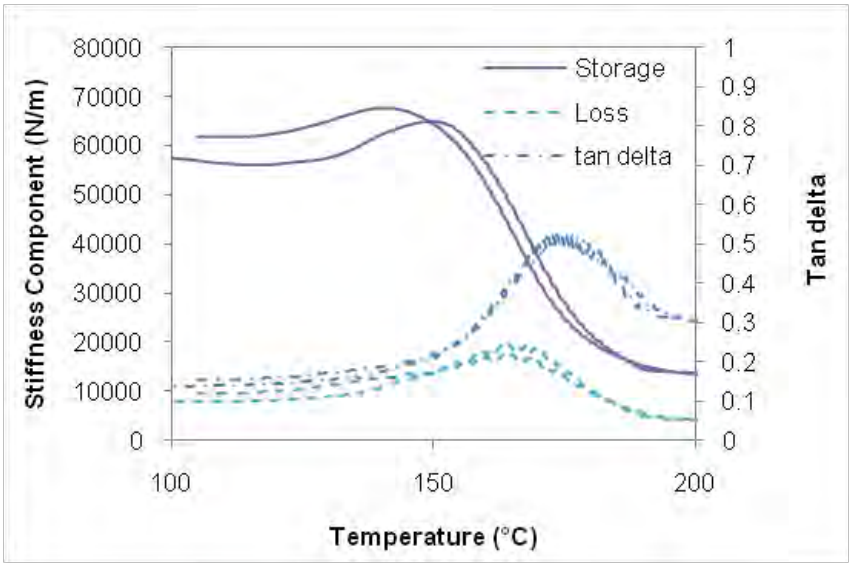

Figure 17. Oscillatory TMA of cured (**11**) after exposure to 85 °C water for 96 hrs.

5.7.4 Single ring cyanate ester composites. After the extensive studies of **10** and **11,** a single ring system with an intermediate length carbon chain, the propyl ester **12** was prepared on a large scale (~35 g). The DSC of this material (Figure 18) showed a favorable melting point of 70 °C allowing for a large processing window. A mixture composed of 15% **11** and 85% **12** was used for the fabrication of both an 8-ply and 16-ply flat panel composite using Hexcel S2-glass fabric as the support (Figure 19)

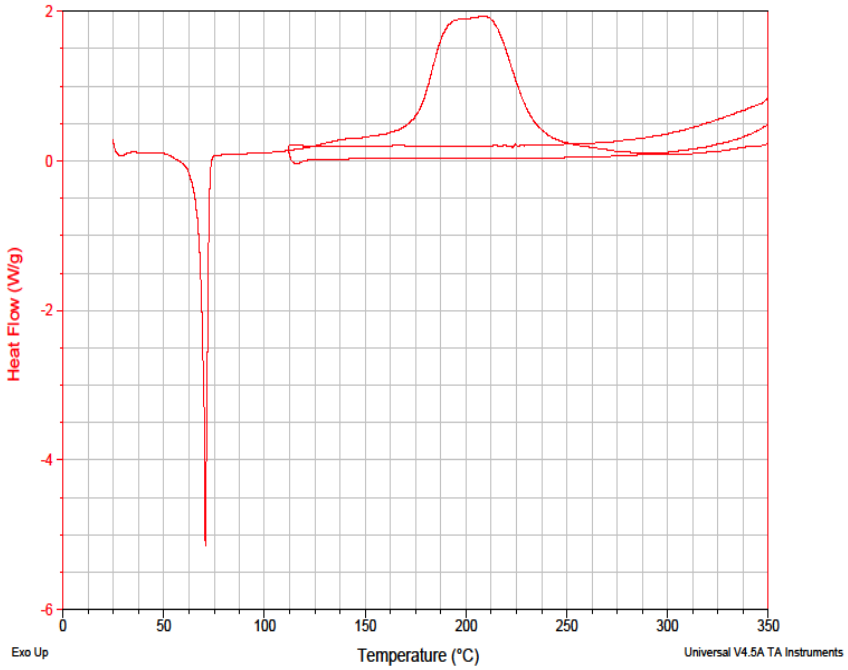

Figure 18. DSC of compound **12**

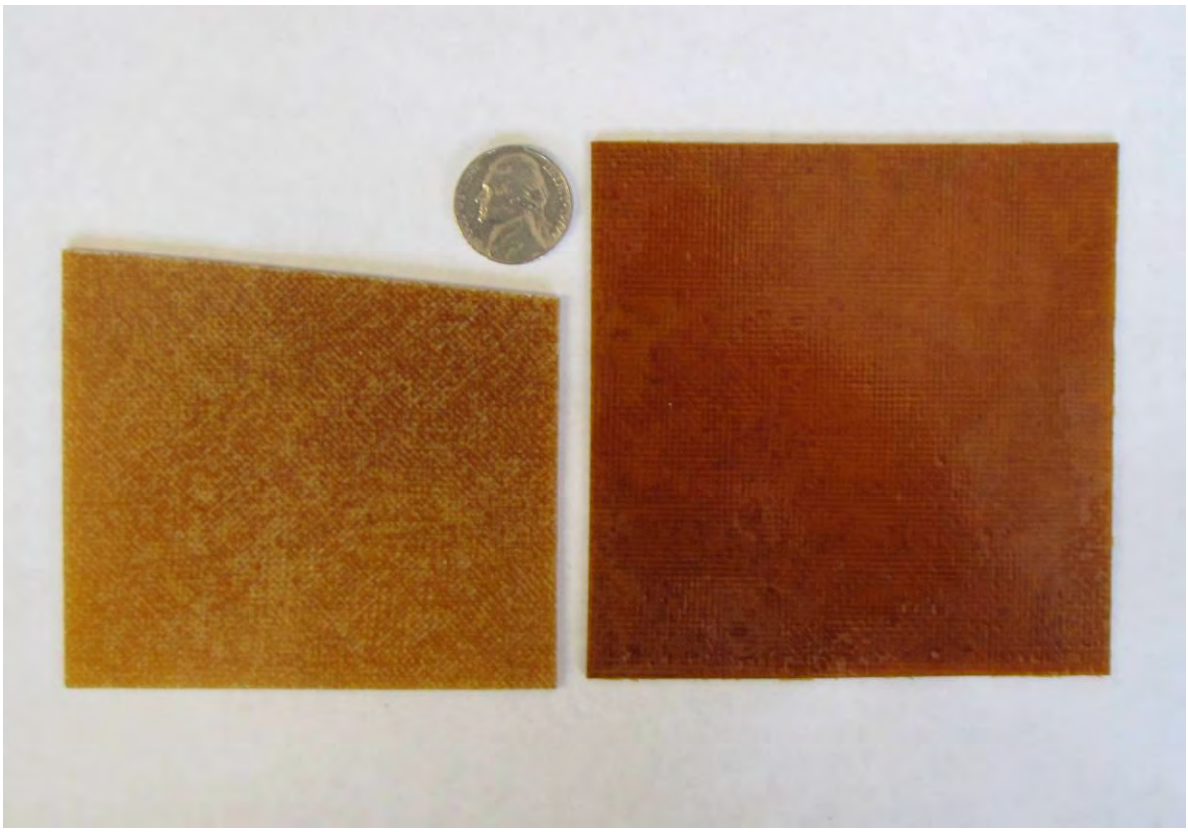

Figure 19. Composite flat panels prepared from compound 12 and supported by Hexcel S2 glass fabric. The panel on the left is a 16-ply specimen, while the sample on the right is 8-ply. The darker color of the right panel is due to a thin layer of Kapton.

5.7.5 Summary of resorcylic derived cyanate esters. Of the two "single ring" cyanate esters studied, **10** had highly desirable moisture uptake characteristics, but it appears that an inability to achieve full cure, combined with a low glass transition temperature, makes this material unsuitable for most applications. An exception may be radomes, where the low water uptake and stability of T_g on extended exposure to moisture could lead to very low and stable dielectric properties. The thermal ceiling temperature of any such radomes, however, would be limited to 200 °C for short-term use due to the possibility of CO_2 generation from the uncured cyanate ester groups at or above this temperature, and most likely to 120 °C for long-term use due to the low T_g. State-of-the-art composites made from ultrahigh modulus polyethylene fibers that are often employed in electronic equipment are already limited by the fiber's mechanical properties to long-term service temperatures of 120 °C, however. Despite potential limitations, **10** did reveal a potentially quite interesting and unexplored aspect of thermosetting cure chemistry, namely the idea that additional cure in such systems could be induced by simply swelling with water.

11 shows some promise as a high-temperature resin, however, in order to provide adequate dimensional stability, the moisture uptake will need to be reduced by at least a factor of two. Such reduction likely can be achieved by reducing the density of cyanurate rings, at a likely cost of 50 -100 °C in dry T_g. This decrease in dry T_g would likely still yield acceptable

thermomechanical stability in dry environments for many aerospace applications. If the decrease in water uptake also led to an improved "wet" T_g, then a viable replacement for many catalyzed cyanate ester systems could be attained. A significant remaining issue for future study, however, would be the storage stability of this self-catalyzing material. Many commercial aerospace resins, though, require storage at -20 °C, so while the shelf life issue is important, the odds are reasonably good that it can be successfully managed.

5.8 Renewable tricyanate esters

As the final thrust of our research, we investigated synthetic routes to produce tricyanates from readily available natural products. Anisyl alcohol ((4-methoxyphenyl)methanol) which can be found in anise, honey, bourbon, and vanilla was chosen as a promising starting point. The chlorinated version, 1-(chloromethyl)-4-methoxybenzene was readily converted to **14** by treatment with triethylphosphite. Coupling of **14** with 3,5-dimethoxybenzaldehyde then leads to **15**. Hydrogenation of **15** gives saturated **16**, while cleavage of the methyl ethers yielded **17** which was converted to the cyanate ester **18** by treatment with cyanogen bromide and triethylamine (Scheme 10). An ORTEP derived from a single crystal X-ray diffraction study and a photo of typical crystals can be seen below (Figure 20). Through this work

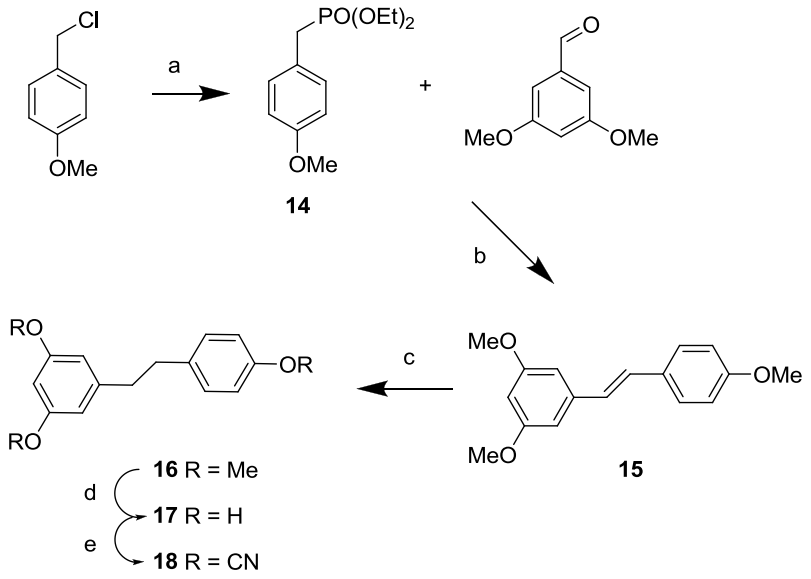

Reagents & conditions: a) $P(OEt)_3$, reflux; b) KO*t*Bu, THF, reflux;
c) H_2, Pd/C, EtOH; d) pyridine HCl, 180°C; e) BrCN, TEA, acetone, - 10°C.

Scheme 10. Synthesis of a tricyanate ester from 1-(chloromethyl)-4-methoxybenzaldehyde

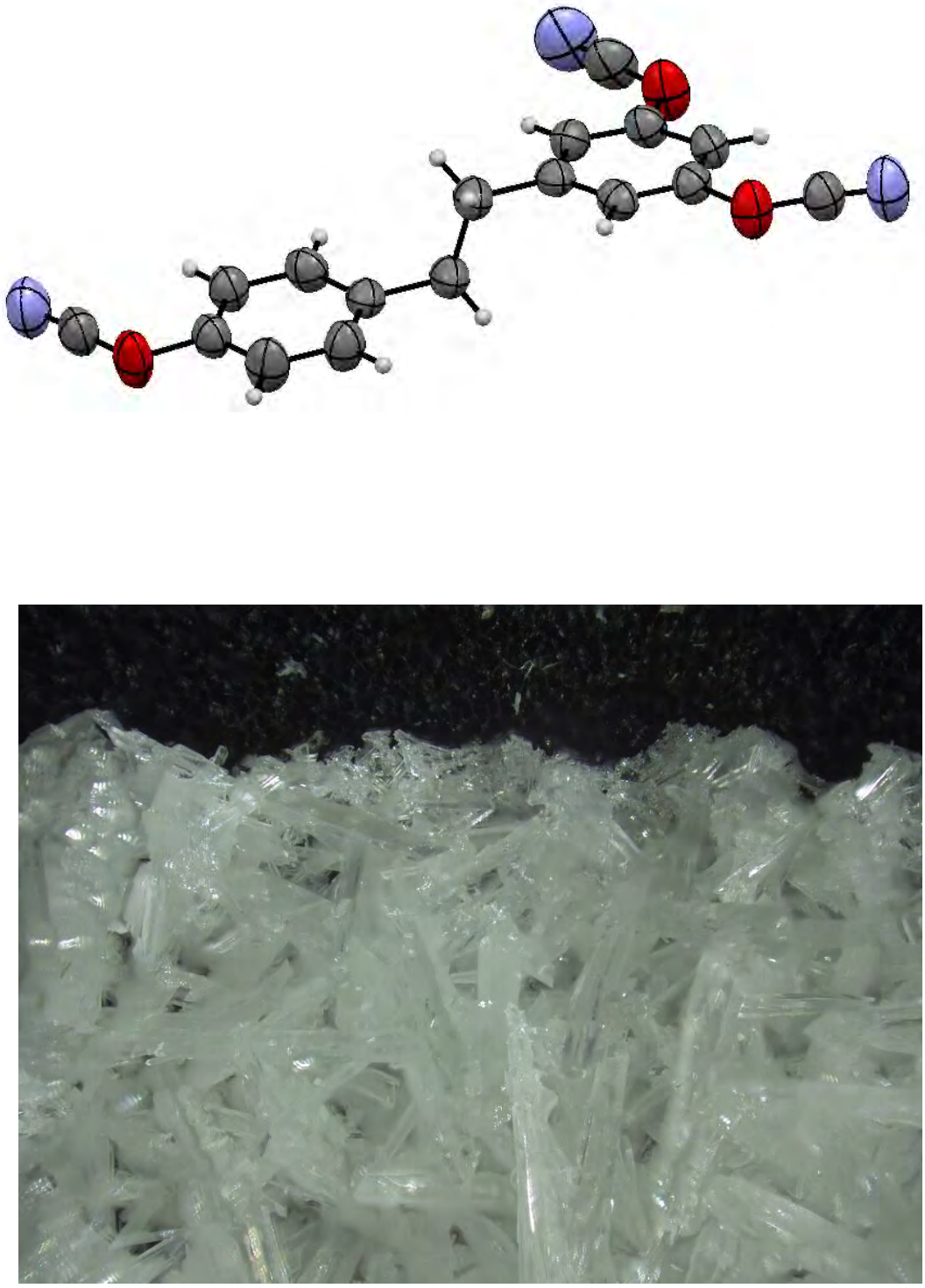

Figure 20. ORTEP of Compound **18** (top) and composite photograph (bottom) of the typical product derived from crystallization of the extraction solvent.

it was shown that a tricyanate ester could be efficiently constructed from simple renewable phenols. Food grade resveratrol can also be purchased commercially and hydrogenation followed by reaction with cyanogen bromide and triethylamine allowed for a two step preparation of **18**. This latter method was optimized and was successfully run on up to a 12 g scale. Key advantages of this latter synthesis include a purification process that accomplishes both the extraction and crystallization of the material in one step with the environmentally favorable solvent ethyl acetate. A DSC of **18** (Figure 21) shows a modest melting point of 120 °C which allows for a large processing window. TMA data is currently being collected on resin samples and work is proceeding on the fabrication of flat panels. **18** may have key advantages over bis-cyanate esters due to the potential for a higher cross-link density coupled with a flexible linkage between rings. This combination may produce both a high T_g and improved toughness.

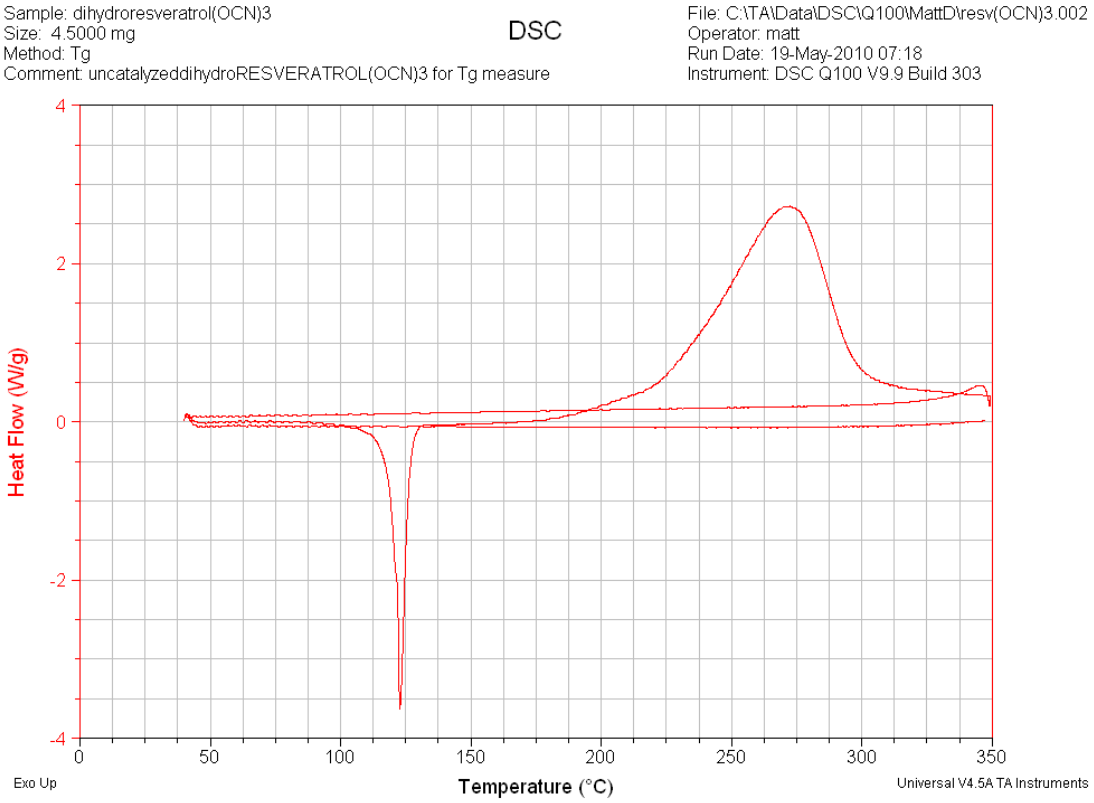

Figure 21. DSC of compound **18**

6. Concluding Remarks

6.1 Project Summary

In this limited scope proposal we have developed several routes to renewable, high performance cyanate esters. In our first approach we focused on a complex mixture of phenols extracted from the creosote bush. This method has advantages including a simple extraction procedure, isolation of a liquid product that should facilitate straightforward fabrication processes, and the ability to produce resin in one step from the extract. Unfortunately, we also discovered several disadvantages including an unpredictable pot life for the resin and an inconsistent distribution of phenols and resin behavior depending on the source of the extract. This variability may significantly limit the use of these crude extracts as resin precursors.

In the second route, we developed efficient methods for both the oxidative and reductive coupling of vanillin to produce *bis*-phenols and subsequently *bis*-cyanate esters. The oxidative coupling method produced a resin that did not fully cure, likely due to steric hindrance. In contrast, the reductive coupling route produced a resin that underwent complete cure and had a T_g of 202 °C. In addition, the decomposition of these materials was evaluated by TGA/FTIR. These studies showed that decomposition of methoxy-substituted cyanate esters occurred well above 300 °C suggesting that their presence will not have a significant impact on the use temperatures of these materials. In addition to the results detailed in this report, we have recently done some preliminary studies in which we have demonstrated the feasibility of an electrochemical approach to produce saturated bis-phenols from vanillin. This method has advantages including scalability and the use of environmentally favorable solvents such as water and acetic acid. We have also developed a method for the oxidative coupling of vanillin utilizing the enzyme horseradish peroxidase with hydrogen peroxide. To address other thermoplastics, work is currently proceeding on the synthesis of renewable polycarbonates in addition to cyanate esters.

In the third route, we synthesized three different single ring bis-cyanate ester resins from α-resorcylic acid. Through this work we showed that the T_g and water uptake of these resins could be elegantly controlled through the introduction of various alkyl groups via condensation reactions with the carboxylic acid. We were also able to fabricate two different flat panel composites (cyanate ester/glass fiber) with the propyl functionalized resin.

In the fourth and final route, a tricyanate ester was synthesized both from renewable single ring precursors and directly from hydrogenated resveratrol. Thermal analysis of the saturated resin shows that it may be a suitable candidate for fabrication of composite flat panels. The use of a tricyanate as compared to a dicyanate may also impart advantages such as increased T_g while maintaining suitable toughness.

This limited scope proposal has shown that several viable alternatives to petroleum derived resins can be produced from renewable and sustainable phenolic compounds. The creation of a variety of promising candidates has greatly reduced the risk of our approach and will allow for custom tailoring of renewable cyanate ester resins on the basis of physical properties, environmental impact, cost, and ease of composite fabrication. In turn, this versatility will allow for these resins to be used in diverse environments and on an eclectic set of DoD platforms.

6.2 Future Directions

6.2.1 Vanillin derived resins. Three key areas of research are proposed to reduce the environmental impact of these resins, improve their performance, and facilitate the fabrication of composites. First, we have recently shown that the reductively coupled product can be produced through a two-stage electrochemical process. Both stages need to be optimized and the reductive step needs to be better understood. Second, using 4-methyl-2-methoxyphenol as a starting point, a variety of *bis*-phenols can be constructed through condensation with various renewable aldehydes and ketones. In particular, the linkage between phenols can be constructed in a manner that allows for elegant control over the melting point of the cyanate ester. Cyanate esters that have melting points under 100 °C and particularly under 50 °C are much easier to incorporate into composites and the ability to produce resins with low melting points will greatly reduce the complexity and cost of the fabrication process. Third, in the course of synthetic work completed under this limited scope project, methods were optimized for the efficient conversion of methoxy-groups to phenols. This conversion process coupled with an initial step to eliminate the starting phenol will allow for new *meta*-*bis*-phenols with reduced steric limitations, improved thermal stability, and higher T_g's. This same technique can be used for phenols produced through condensation with aldehydes and ketones.

6.2.2 Resorcylic acid based resins. Although we have already shown that these resins are promising candidates for high performance composites, our starting point, α-resorcylic acid is only a model compound and not a major product derived from the reaction of resorcinol with alkali carbonates. Instead, the phenols direct the carbonate to the *ortho* and *para* positions of the ring. To address this issue, we will synthesize bis-phenols directly from resorcinol. Either mixtures, or depending on the ease of separation, pure monomers will then be cyanated and fully characterized. Although the new isomers will have subtly different steric and electronic properties, it is not expected that significant variations in T_g, thermal stability, or water uptake will result.

6.2.3 Tricyanate ester resins. All of the synthetic work for resveratrol has already been completed. More than 35 g of the tricyanate has been prepared and is awaiting further testing. At this point the T_g of this material is unknown and a flat panel has not yet been prepared. The completion of these tasks will determine the utility of resveratrol derived cyanate esters.

6.2.4 Flat panel fabrication and testing. In the current work, flat panels were prepared only from compound **12**. Future efforts would focus on the development of optimized fabrication processes to produce panels from several different materials. Key properties including toughness, water uptake, and thermal stability will be evaluated.

7. References

1. Landman, D. *Developments in Reinforced Plastics Vol. 5*, ed. G. Pritchard; Applied Science; London: **1986**, p. 39.
2. Shimp, D. A. *Chemistry and Technology of Cyanate Ester Resins*, ed. I. Hamerton; Blackie Academic, New York: **1994**; pp. 282-328.
3. Snow, A. W. *Chemistry and Technology of Cyanate Ester Resins, ed. I.* Hamerton; Blackie Academic, New York: **1994**; pp. 7-57.
4. Ramachandra, R. S.; Ravishankar, G. A. *J. Sci. Food Agric.* **2000**, *80*, 289-304 and references cited therein. Methods to accelerate this process have been investigated: Dignum, M. J. W.; Kerlera, J.; Verpoorte, R. *Food Rev. International* **2001**, *17 (2)*, 119–120. For biotechnological production routes to vanillin see: Priefert, H.; Rabenhorst, J.; Steinbüchel, A. *Appl. Microbiol. Biotechnol* **2001**, *56*, 296-314 and references cited therein.
5. Krings, U.; Berger, R. G. *Appl. Microbiol. Biotechnol.* **1998**, *49*, 1-8 and references cited therein.
6. Biosynthetic routes to guaiacol have also been explored. See: Duffey, S. S.; Aldrich, J. R.; Blum, M. S. *Comparative Biochemistry and Physiology, Part B: Biochemistry & Molecular Biology* **1977**, *56 (2B)*, 101–102.
7. Esposito, L. J.; Formanek, K.; Kientz, G.; Mauger, F.; Maureaux, V.; Robert, G.; Truchet F. *Kirk-Othmer Encyclopedia of Chemical Technology, 4th ed*., **1997** New York: John Wiley & Sons, pp. 812–825.
8. Boerjan, W.; Ralph, J.; Baucher, M. *Ann. Rev. Plant Biol.* **2003**, *54*, 519–549.
9. Hocking, M. B. *J. Chem. Edu.* **1997**, *74(9),* 1055–1059 and references cited therein.
10. Lignin produced as part of a biofuel refining operation often produces a cleaner and more consistent lignin product. For a general treatment see: Zhang, Y.-H. P. *J. Ind. Microbiol. & Biotechnol.* **2008**, *35*, 367-375 and references cited therein.
11. For example see: Voitl, T.; Rudolf von Rohr, P. *Chem. Sus. Chem. **2008,*** 1(8-9), 763-769.
12. Pickering, S. J. *Composites Part A: Applied Science and Manufacturing* **2005**, *37*, 1206-1215
13. Buttke, K.; Niclas, H.-J. *Prakt. Chemie/Chemik.-Zeit.* **1998**, *340(7)*, 669-675.
14. Guenthner, A. J.; Yandek, G. R.; Mabry, J. M.; Lamison, K. R.; Davis, M. C.; Cambrea, L. R. *Proceedings of SAMPE '10*, Vol. 55 (Covina, CA: SAMPE International Business Office, 2010), paper 42ISTC-119.
15. CRC Handbook of Chemistry and Physics, 82nd ed, (David R. Lide, ed.; Boca Raton, FL: CRC Press, 2002, p 8-60.
16. For a general treatment of high-performance polymers based on cyanate esters see: *Chemistry and Technology of Cyanate Esters,* Hamerton, I. Ed.; Chapman and Hall: Glassgow, **1994**. Hamerton, I.; Barton, J.M.; Chaplin, A.; Howlin, B.J.; Shaw, S.J. *Polymer* **2001**, *42*, 2307-2319 and references cited therein.
17. Wang, Q.; Yang, Y.; Li, Y.; Yu, W.; Hou, Z.J. *Tetrahedron* **2006**, 62, 6107-6112
18. General aryl-aryl coupling methods: Bolm, C.; Legros, J.; Paih, J. L.; Zani, L. *Chem. Rev.* **2004**, *104*, 6217. Diaz, D. D.; Miranda, P.O.; Padron, J. I.; Martin, V. S. *Curr. Org. Chem.* **2006**, *10*, 457
19. Marques, F.A.; Simonelli, F.; Oliveira, A.R.M.; Gohr, G.L.; Leal, P.C. *Tet. Lett.* **1998**, *39*, 943-946.

20. McMurry, J. E.; Fleming, M. P. *J. Am. Chem. Soc.* **1974**, *96*, 4708-4709. Mukaiyama, T.; Sato, T.; Hanna, J. *Chem. Lett.* **1973**, 1041-1044. Tyrlik, S.; Wolochowicz, I. *Bull. Soc. Chim. Fr.* **1973**, 2147-2148. For a general treatment of the topic see: McMurry, J.E. *Chem. Rev.* **1989**, *89*, 1513-1524 and references cited therein.
21. For related x-ray structural data on cyanate esters see: Guenthner, A.J.; Yandek, G. R.; Wright, M.E.; Petteys, B. J.; Quintana, R.; Connor, D.; Gilardi, R.D.; Marchant, D. *Macromolecules* **2006**, *39(18)*, 6046-6053 and references cited therein.
22. Guenthner, A. J.; Yandek, G. R.; Mabry, J. M.; Lamison, K. R.; Davis, M. C.; Cambrea, L. R. "Insights into moisture uptake and processability from new cyanate ester monomer and blend studies" *Proceedings of SAMPE 10,* Vol. 55 (Covina, CA: SAMPE International Business Office, 2010), in press.
23. Yan, H.Q.; Chen, S.; Qi, G. R. Polymer 2003, 44, 7861-7867
24. Pascault, J.P.; Williams, R.J.; J. Polym. Sci. Polym. Phys. 1990, 28, 85.
25. Bicerano, J. Prediction of Polymer Properties, 3rd Ed. (New York: Marcel Dekker Inc.) , 2002.
26. Chemistry and Technology of Cyanate Ester Resins; Hamerton, I., Ed.. (London, UK: Chapman & Hall), 1994.
27. Wright, M. E.; Petteys, B. J.; Guenthner, A. J.; Yandek, G. R.; Baldwin, L. C.; Jones, C.; Roberts, M. J. "Synthesis and Chemistry of a Monotethered-POSS Bis(Cyanate Ester): Thermal Curing of Micellar Aggregates Leads to Discrete Nanoparticles", *Macromolecules*, 40, 3891-3894 (2007).